COMPARATIVE ANALYSES OF CHLAMYDIA INFECTION IN WILD TYPE MICE AND MICE WITH EPITHELIAL AUTOPHAGY DEFICIENCY

By

LAUREN BATTAGLIA

A thesis submitted to the Graduate School- New Brunswick

Rutgers, The State University of New Jersey

and

The Graduate School of Biomedical Sciences

University of Medicine and Dentistry of New Jersey

In partial fulfillment of the requirements

For the degree of

Master of Science

Graduate program in Cell and Developmental Biology

Written under the direction of

Dr. Huizhou Fan

and approved by

_____

_____

_____

New Brunswick, New Jersey

October 2013

ABSTRACT OF THE THESIS

Comparative Analysis of *Chlamydia* Infection in Wild Type Mice and Mice with Epithelial Autophagy Deficiency

By LAUREN BATTAGLIA

Thesis Director:
Dr. Huizhou Fan

Chlamydia is the most common cause of sexually transmitted bacterial infection worldwide and it leads to severe complications for women who become infected. Following initial infection, the bacterial pathogen ascends from the lower genital tract to the upper genital tract leading to pelvic inflammation and scarring of inflamed tissue. The scarring can lead to ductal obstruction, causing retention of fluid in the upper genital tract and ovaries, termed hydrosalpinx. This inflammation due to *Chlamydia* infection can lead to infertility. Despite the commonality of the disease and its severe consequences, the molecular pathogenesis and mechanism of pelvic inflammation following Chlamydia infection has yet to be elucidated. We investigated the molecular pathogenesis and its relation to host autophagy here.

The ATG5 gene is required for autophagy. Our lab has previously shown via mouse model that deletion of the ATG5 gene in myeloid cells results in a significant increase in upper genital tract inflammation following Chlamydia infection. To further investigate the role of autophagy in Chlamydia pathogenesis, mice with deleted ATG5 gene in epithelial cells were intravaginally infected with *Chlamydia*. The infection was monitored through weekly vaginal swabbing and calculation of *Chlamydia* bacterial titers from each swab. After *Chlamydia* infection cleared, the animals were sacrificed, upper genital tract pathology was observed and cytokine analysis was conducted on the vaginal swabs that were taken throughout the infection.

The p62 autophagy protein acts as a scaffold to bring bacterial pathogen to autophagy machinery. In the current study, p62-deficient mice were obtained and infected with *Chlamydia*. Vaginal swabbing throughout *Chlamydia* infection allowed

us to estimate bacterial titers and assay the host cytokine response to the infection, and finally the upper genital tracts of the animals were removed for observation.

We found no significant difference in the pathology, bacterial clearance, or cytokine analysis between epithelial Atg5-deficient animals and wild type animals. This suggests that the *Chlamydia* bacteria may be employing mechanisms to evade or inhibit host autophagy in epithelial cells to promote its own survival. Additionally, there was no significant difference in the pathology, bacterial clearance, or cytokine analysis between the p62-deficient animals and wild type animals.

ACKNOWLEDGMENT

I would first like to thank my thesis advisor Dr. Huizhou Fan for all of his help and guidance during my time at UMDNJ and Rutgers. His expertise in the area of *Chlamydia* research allowed me to learn and grow as a scientist as I worked to complete my project. Dr. Fan not only encouraged me to explore science through research, but he also generously offered his support and assistance as I worked toward my future career goals in medicine. I would also like to thank the other members of my thesis committee for their thoughtful suggestions.

Eddie Kang, Xiaofeng Bao, and Lingling Wang I would like to thank for offering their guidance and expertise to help me complete my project. They have helped me learn numerous new techniques, and they have enthusiastically answered all of my questions as I have progressed through this project.

I would finally like to thank Henry and my parents for their continued support and encouragement. Even when I have been unsure if I would reach my goals, they have always been there to listen and offer motivation, and without them I would not be where I am today.

TABLE OF CONTENTS

LIST OF FIGURES

LIST OF ABBREVIATIONS

APC	Antigen Presenting Cell
ATG5	autophagy protein 5
BSA	bovine serum albumin
DAMP	danger-associated molecular pattern
EB	elementary body
ELISA	enzyme linked immunosorbant assay
ER	endoplasmic reticulum
IFU	inclusion forming units
IgA	immunoglobulin A
IgE	immunoglobulin E
IgG2	immunoglobulin G2
IgG4	immunoglobulin G4
IgM	immunoglobulin M
IL-1α	interleukin 1α
IL-2	interleukin 2
IL-6	interleukin 6
IL-17	interleukin 17
LAMP1	Lysosomal-associated Membrane Protein 1
LC3	1A/1B-light chain 3
LLPD	long-lived protein degradation
MEF	mouse embryonic fibroblast
MHC-II	Major Histocompatibility Complex – Class II
MoPn	Mouse Pathogen *C. Muridarum*
mTOR	mammalian target of rapamycin
NFκB	nuclear factor-κB
PAMP	pathogen-associated molecular pattern
PBS	phosphate buffered saline
PID	Pelvic inflammatory disease

RB	reticulate body
T3SS	type 3-secretion system
T_H Cell	T-Helper Cell
TNF-α	tumor necrosis factor-α
UGT	Upper Genital Tract
WT	Wild Type

CHAPTER 1

INTRODUCTION

Chlamydia is an obligate intracellular bacteria that reportedly causes more cases of sexually transmitted infection (STI) worldwide than any other bacterial pathogen [1]. The name *Chlamydia* is derived from the Greek word meaning "cloak," [2] an etymology that is fitting of the infection since *Chlamydia* is often protected, or 'cloaked,' by an asymptomatic infection. As a result, many *Chlamydia trachomatis*-infected individuals do not seek treatment even in parts of the world where there is access to good healthcare. Although the infection may be deceptively symptomless, *Chlamydia* remains a major public health concern due to the severe long-term complications of infection, especially in women. The long-term dangers of *Chlamydia* infection include salpingitis, pelvic inflammatory disease (PID), chronic pain, and ectopic pregnancy. *Chlamydia* infection may also lead to infertility in men and women [3]. *C. trachamatis*, which can be passed to infants born to mothers infected with *Chlamydia*, infects the upper eyelids and cornea and is the world's most common infectious cause of blindness [1]. The WHO reports that there are 3-4 million new cases of *C. trachomatis* infection each year in the USA alone, and in some parts of the developing world over 90% of individuals are infected [1]. Furthermore, *Chlamydia pneumoniae* is a common respiratory pathogen that is believed to

contribute to atherosclerosis [4, 5], and may also play a role in asthma [6, 7] and neurodegenerative diseases including Alzheimer's disease [8-10].

Due to the prevalence and severity of *Chlamydia* infection worldwide, *Chlamydia* is becoming an important area of scientific research. *Chlamydia* invade cells by binding to the surface of the cell and entering via a vacuole that is called the *Chlamydia* "inclusion." Within the inclusion, the pathogenic form of *Chlamydia*, called the elementary body (EB), differentiates into the metabolically active form of *Chlamydia*, or the reticulate body (RB), and replicates so that the pathogen can go on to infect more host cells. One way the host responds to *Chlamydia* infection is through autophagy, or the engulfment of the *Chlamydia* inclusion. The mechanism of autophagy involves the formation of a double-membrane called the "isolation membrane" around unwanted cellular material or an invading pathogen within a cell. The isolation membrane extends around the intracellular bacteria, enveloping it in a vesicle called the "autophagosome," which then fuses with a lysosome so that its contents can be degraded. It is understood that epithelial cells are the chief target of *Chlamydia* [3, 11]. Interestingly, previous studies have shown that the *Chlamydia* inclusion does not fuse with the epithelial lysosome [12-16], but the lysosomes of blood monocytes and neutrophils are active in degrading the invading *Chlamydia* elementary bodies [11, 17-19]. This suggests a possible mechanism by which *Chlamydia* evades host epithelial autophagy. More investigation to gain a better understanding of the interplay between *Chlamydia* and host autophagy may pave the way for new therapeutic targets against *Chlamydia*.

As they have evolved, other bacterial pathogens are known to have developed mechanisms to evade or inhibit the host autophagy in order to promote their own survival [11, 20, 21]. For example, *Coxiella burnetti*, the bacteria that causes Q fever, evolved the ability to survive and grow within a lysosomal environment [11, 22]. *Mycobacterium tuberculosis* developed a mechanism to adjust its vacuole membrane, preventing fusion with the autophagosomes and thus inhibiting autophagy [11, 23]. It has yet to be determined specifically how *Chlamydia* and host autophagy interact. However, previous studies have indicated that *Chlamydia* infection stimulates host autophagy machinery, as demonstrated by significant elevations in the levels of autophagy marker LC3-II following *Chlamydia* infection and increased colocalization of LC3 with lysosomal marker LAMP1 [24]. Previous research has also shown that increased LC3-II expression in MEFs and HeLa cells following *Chlamydia* infection was accompanied by no change in p62 expression, although p62 expression would be expected to decrease if autophagy were working to completion because p62 is degraded in the process of autophagy [11]. Taking into account the ability of other bacterial pathogens to evade host autophagy and the apparent failure of autophagy to reach completion in cells infected with *Chlamydia*, the interaction between *Chlamydia* and host autophagy machinery becomes a worthwhile topic for further research. Our lab has worked to understand regulation of host autophagy by *Chlamydia in vitro* and obtained data that suggest *Chlamydia* does block autophagy completion in the lysosomes of infected cells [11].

In order to explore the implications of host epithelial autophagy for *Chlamydia in vivo*, we developed a mouse line with the autophagy gene Atg5

knocked out specifically in the genital epithelial cells. These mice were intravaginally infected with *C. trachomatis* alongside control mice capable of epithelial autophagy, and we were able to monitor the progression of the infection through weekly vaginal swabbing of the mice.

Specific Aims

Aim 1: To determine if genital epithelial Atg5 gene knockout mice have an altered ability to clear bacterial load after *Chlamydia* infection as compared with wild type mice.

Rationale: While the exact molecular interaction between host epithelial autophagy machinery and *Chlamydia* has not yet been elucidated, it has been shown that *Chlamydia* is capable of blocking the completion of autophagy in epithelial cells [11]. Therefore, it will be informative to explore and compare the ability of autophagy-deficient mice and wild type mice to clear *Chlamydia*.

Aim 2: To determine if epithelial Atg5 gene knockout mice experience a change in regulation of inflammatory cytokines after *Chlamydia* infection as compared with wild type mice.

Rationale: It has been suggested that *Chlamydia* evades, down-regulates, or blocks the completion of host epithelial autophagy to promote bacterial survival. In order to examine the host response to *Chlamydia* infection, it is worthwhile to investigate whether there is a difference in inflammatory cytokine response between wild type

versus autophagy-deficient mice infected with *Chlamydia*. If *Chlamydia* evades host epithelial autophagy, there will be no significant difference in cytokine response between wild type and epithelial autophagy-deficient animals.

Aim 3: To establish whether there is a significant difference in physiology between the epithelial Atg5 gene knockout mice and the wild type mice after intravaginal infection with *Chlamydia*.

Rationale: Uterine horn dilation and oviduct hydrosalpinx are known facets of urogenital tract pathologies caused by vaginal *Chlamydia*l infection in mice [25]. Furthermore, our lab has demonstrated that *Chlamydia*-infected mice with autophagy-deficiency in myeloid cells are significantly more likely to develop severe upper genital tract pathology than wild-type animals (unpublished). It is worthwhile to investigate whether knocking out the autophagy mechanism specifically in epithelial cells affects the mouse physiology and pathology of the disease.

CHAPTER 2.

REVIEW OF THE RELATED LITERATURE

Chlamydia **Developmental Cycle**

Chlamydia exists in two distinct cellular forms, namely the infectious elementary body (EB) and the proliferative reticulate body (RB) [11, 26, 27]. To begin the developmental cycle, the EB binds to a eukaryotic host cell and is taken into a vacuole within the cell via endocytosis. The vacuole is now called an "inclusion". Within the inclusion, the EB differentiates into the RB, which is metabolically active but noninfectious. The RB replicates and accumulates within the inclusion, and eventually the many RBs reorganize back into the EB cellular form. The EBs are finally released from the host cell and go on to infect more host cells [11, 26, 27].

Chlamydia **pathology**

Chlamydia infection is known to propagate a characteristically chronic, severe inflammation of the upper genital tract that leads to damage to the epithelium. The inflammation is caused by an influx of polymorphonuclear neutrophils and lymphocytes into the genital tract [3]. As the infection progresses, plasma cells and macrophages are recruited to the site of inflammation [3]. Eventually lymphoid follicles that contain B cells and macrophages at their center and T cells at their periphery develop in the inflamed genital tract [3]. Epithelial cells, which are the

primary target of *Chlamydia* [11, 28, 29], proliferate around the damaged tissue and scar tissue forms [3]. The scar tissue can trap fluid within the upper genital tract, resulting in hydrosalpinx and uterine horn dilation [3].

Due to the existence of multiple serotypes and short-lasting immunity, sexually transmitted *Chlamydia* infection is often recurrent. Repeated infection leads to increased severity of the upper genital tract inflammatory response [3]. Uterine horn dilation and oviduct hydrosalpinx are characteristic urogenital tract pathologies that result from vaginal *Chlamydia* infection in mice [25]. In some human patients, *Chlamydia* persistence is maintained for years [3]. *Chlamydia* infection stimulates host immune machinery to secrete proinflammatory cytokines, chemokines, and growth factors [3]. However, microbial persistence may arise when the immune system is incapable of clearing the entire infection, allowing the bacteria to chronically infect the host. It is possible that the vacuole or "inclusion" in which the RBs multiply serves to protect some of the bacteria from being cleared by the host immune machinery. Additionally, it has been suggested that repeated infection may be due to a shared antigen among *Chlamydia*e that immunologically primes the host, resulting in a type four delayed-type hypersensitivity upon reinfection [3]. The severity of *Chlamydia* infection and the tendency for reinfection underscores a necessity for further research to clarify the host immunological response to the disease.

The Autophagy pathology

'Autophagy' is a term that describes the pathways by which damaged or unwanted cytoplasmic material is delivered to the lysosomes for degradation [21, 30]. The word 'autophagy' literally means "to eat oneself," a name which is appropriate for the process as it often involves the engulfment of a cells' own cytoplasm organelles to be degraded and recycled [31]. Thus, the cell uses autophagy as a go-to pathway for recycling its own materials when nutrients are in short supply. Significantly, autophagy allows the degradation of not only the unwanted cellular material, but also the degradation of unwanted bacterial pathogens that enter the cell. Autophagy is induced to function as a part of the innate immune system in response to the invasion intracellular pathogens [11, 21, 31].

The autophagy pathway may be conceptually divided into three main phases: a nucleation phase, an elongation phase, and a lysosomal fusion phase. First, the nucleation phase is induced by starvation, growth factor deprivation, energy depletion, or an antimicrobial stimulus, leading the protein kinase mammalian target of rapamycin (mTOR) to be inhibited [11, 21, 32]. mTOR inhibition causes the mTOR substrate complex, ATG101 protein that is encoded by autophagy-related genes and RB1CC1 to translocate from the cytosol and associate with specific sites on fragments of endoplasmic reticulum (ER) lipid membrane, helping to facilitate the formation of a short, cup-like complex [11, 32]. The cup-like membrane complex forms around the portions of the cytosol, organelle, or microbe that are to be

degraded. The cup-like membrane complex is termed the 'isolation membrane,' and its lipid membrane components are believed to originate from a segment of the ER membrane [21, 31]. However, some studies have presented evidence that the isolation membrane may also be derived from endosomes, *trans*-Golgi, or even mitochondrial membranes [21].

The second phase of the autophagic pathway is the elongation phase, during which the isolation membrane gradually grows. Autophagy proteins ATG12/ATG5-ATG16L1 dimerize in a conjugated system complex that sits on the outer side of the isolation membrane [21, 33]. Next, a soluble, microtubule-associated protein termed 1A/1B-light chain 2 (LC3-II), which is a marker for autophagy, is recruited to the ATG complex/isolation membrane [11] with the help of the scaffolding protein p62 [34]. This allows fragments of membrane that are likely derived from the endosomal membrane to be added piece-by-piece to the isolation membrane [31, 32]. The elongation phase ends when the isolation membrane has extended long enough for its ends to meet, enveloping its contents within a characteristic double membrane [21, 31, 32]. This double-membraned organelle is called the 'autophagosome.'

Finally, the third phase of the autosomal pathway is one in which the autophagosome, with the help of proteins on its membrane surface, targets and fuses with the membrane of a lysosome via vesicle-tethering proteins [31]. Following lysosomal fusion with the outer membrane of the autophagosome, a single-layer vesicle and its contents are released into the lysosome interior, where lysosomal hydrolases degrade the proteins and lipids that were initially captured by

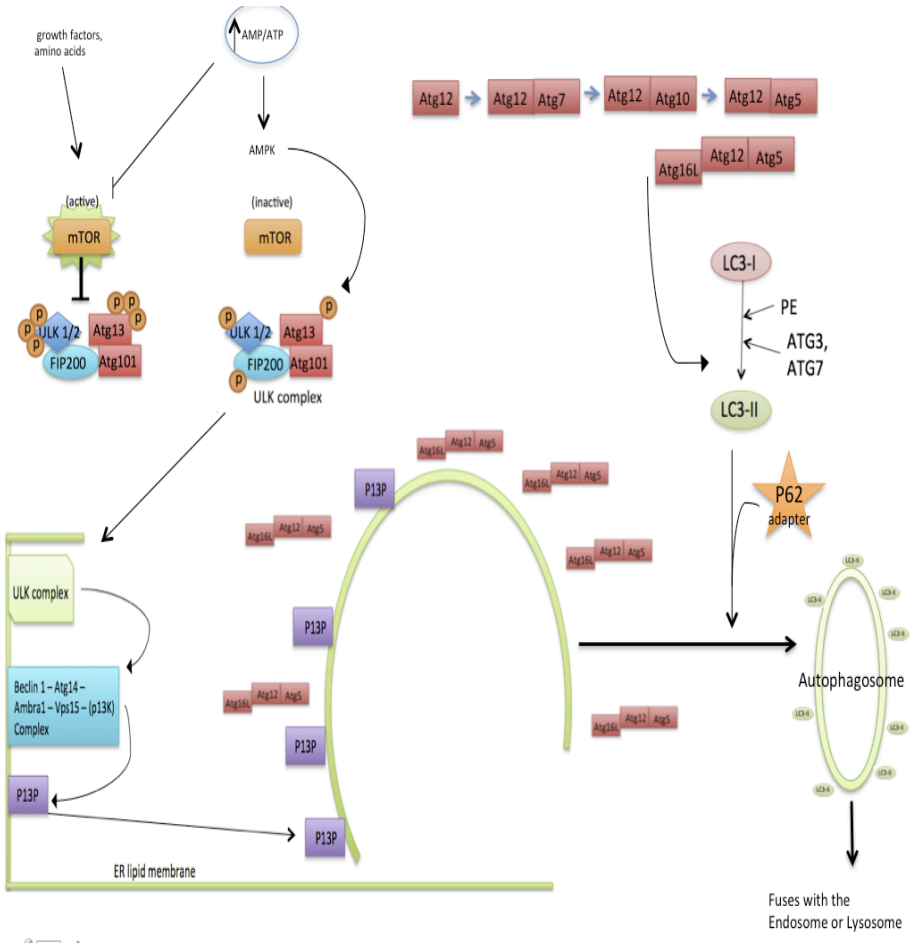

Figure 1. Summary of the autophagy pathway.
The presence of growth factors stimulates the mTOR pathway, which inhibits the ULK complex from becoming activated. In the absence of growth factors or the presence of an immunological stimulus, mTOR is inhibited. This allows the ULK complex to become phosphorylated and activated. The ULK complex triggers the initiation of autophagosome formation from a portion of the ER membrane through a pathway that allows PI(3)P to associate with the fragment of ER membrane.
The Atg pathway is a ubiquitin-like pathway, which results in the formation of the ATG16L-ATG12-ATG5 complex. The ATG16L-ATG12-ATG5 complex associates with the premature autophagosome and promotes elongation. Furthermore, the ATG16L-ATG12-ATG5 complex promotes the lipidation of LC3-I to LC3-II. P62 acts as an adapter protein that allows LC3 to associate with autophagosome. LC3-II is a marker for autophagy that is required for the membrane to complete the elongation phase, resulting in the double-membraned autophagosome that formed around proteins or bacteria that is to be degraded. The autophagosome goes on to fuse with the lysosome, and its contents are released into the lysosome for degradation and recycling.

the autophagosome in the cytosol. The recycled amino acids, lipids, and nucleotides are transported back across the lysosomal membrane and they are ultimately reused by the cell [11, 31]. More and more autophagosomes fuse to the autolysosome until a termination phase in which the lysosome is fragmented and recycled [32]. The autophagy pathway is summarized in **figure 1**.

Role of Autophagy in Infection and Immunity

As discussed above, cells utilize autophagy to defend against intracellular pathogens and parasites. In the cell, everything that is too large to be degraded by the proteasome, including intracellular invading microorganisms like viruses, bacteria, and protozoa, are degraded by autophagy in the lysosome. Additionally, autophagy proteins are essential players in an intricate balancing act that manages the beneficial and detrimental effects of immunity and inflammation. It has been shown that mutation in autophagy genes increases susceptibility to infection by intracellular pathogens [21].

Autophagy is a selective mechanism that specifically targets pathogens and damaged organelles for degradation [35]. In fact, the autophagosome directly interacts with the pathogen-specific, adaptive immune system as shown by its ability to directly interact with not only endosomes and multivesicular bodies, but also major histocompatibility complex (MHC)-class-II loading compartments which exist on the surface of antigen presenting cells (APC's) and carry antigens to stimulate the pathogen-specific cell-mediated immune response [21, 36].

The autophagy protein Atg5 is involved in antiviral, antibacterial, and antiparasitic facets of the immune response. Atg5 autophagy protein additionally assists in antigen presentation, phagosome maturation, apoptotic corpse clearance, T cell and B cell maintenance, and intestinal immune epithelial cell function [21]. Atg5 is essential to the autophagy mechanism; deletion of the ATG5 gene prevents autophagy form occurring.

P62 and Autophagy

P62 is an autophagy protein that acts as an adapter protein between LC3 and the cellular cargo that is to be degraded [34]. P62 plays a key role in the host-defense autophagy mechanism by allowing autophagy machinery specificity when selecting cargo for autophagy. P62 is involved in targeting bacterial invaders to autophagosomes [34]. P62 functions in associating with ubiquitin-coated bacteria-containing vesicles, which is followed by an interaction between p62 and nascent LC3-positive isolation membranes, thus targeting the bacteria-containing vesicles for autophagy [34].

Within the context of *Chlamydia* infection, it has been shown that the expression of p62 protein remained unchanged in HeLa and MEF cells and was increased in *Chlamydia*-infected mouse macrophage RAW cell line [11]. When autophagy functions to completion p62 is degraded in the autolysosome. Therefore, the *Chlamydia*-infected cells would have a decrease in p62 expression if autophagy were functioning to completion [11]. The unchanged and increased p62 expression detected in this study strongly indicates that autophagy is either blocked from

functioning to completion following *Chlamydia* infection or blocked from being upregulated following *Chlamydia* infection. Additionally, no colocalization of p62 with L2 was detected in this study, suggesting a possible inability of p62 to recognize *Chlamydia* and direct it to the autophagy machinery. While p62 is not the only adaptor protein that can bind intracellular bacteria, it has yet to be determined whether other adaptor proteins are capable of recognizing *Chlamydia* [11].

Interestingly, p62 is involved in autophagy beyond the targeting of intracellular pathogens for autosomal degradation. *Shigella* vacuolar membrane remnants generated by T3SS-dependent membrane damage are targeted by polyubiquitination, p62, and LC3 for autophagosomal degradation [21, 37]. If membrane remnants are allowed to accumulate, the immune machinery that functions in sensing intruders through pathogen-associated molecular pattern (PAMP) and danger-associated molecular pattern (DAMP) signals, leading to an increase in NF-κB (nuclear factor-κB)-dependent cytokine production. All of this leads to potentially damaging downstream inflammation. Therefore, the ubiquitin-p62-dependent autophagic targeting of pathogen-damaged membranes may assist in controlling the potentially detrimental downstream inflammatory signaling during bacterial invasion of host cells.

IL-1, IL-4, IL-5, IL-6, IL-17, TNF-alpha Cytokines

Cytokines are small proteins with a molecular mass of ~25kDa that are produced and secreted by a cell in response to external stimulus, and they can affect other

cells by binding to a specific cell-surface receptor [38]. IL-6, TNF-alpha, and IL-1 are pro-inflammatory cytokines that are secreted by macrophages and can be localized to a particular infected tissue, or manifested systemically throughout the body [38]. Systemically, IL-1, IL-6, and TNF-alpha cause fever, or rise in body temperature, that helps the immune system fight infection and helps reduce pathogen replication. Additionally, IL-1, IL-6, and TNF-alpha enhance an acute-phase response in which soluble plasma proteins are secreted by hepatocytes in the liver that help complement, a component of the innate immune response, fix onto pathogen surfaces [38].

IL-4 and IL-5 are cytokines that are secreted by T-Helper Cells (T_H cells) following an infection. By promoting heavy chain isotope switching, IL-4 and IL-5 induce naïve B cells to differentiate into plasma cells that secrete a variety of immunoglobulins including IgM, IgG2, IgG4, IgA, and IgE [38]. Each immunoglobulin takes on a specific role in fighting infection. Following *Chlamydia* infection, one would expect the secretion of IL-4 and IL-5 to be elevated in order to promote immune response [38, 39].

Some helper CD4 T cells secrete a large amount of cytokine IL-17, and these are termed T_H17 cells. IL-1 assists in the development of this subpopulation of CD4 T cells. T_H17 cells function in promoting a state of inflammation: IL-17 binds to the IL-17 receptor on epithelial cells and induces the secretion of cytokines that recruit inflammatory cells to the site of infection [38].

Conclusion

Chlamydia is a serious health concern across the globe. It has been shown that *Chlamydia* may be able to employ mechanisms to evade host autophagy in order to promote bacterial survival [11]. However, unpublished data in our lab demonstrated a significantly more severe pathology in *Chlamydia*-infected mice without autophagy in myeloid cells than in wild-type mice. In order to reveal a broad picture of the *Chlamydia* disease with relation to autophagy in epithelial cells, we investigated the bacterial titers, pathology, and cytokine levels in wild type and epithelial autophagy-deficient mice following *Chlamydia* infection. We also collected bacterial titers, pathology data and cytokine data from wild type and p62-deficient mice. A better understanding of the interaction between autophagy machinery and *Chlamydia* may reveal new therapeutic targets, thus helping to pave the way for new treatments against *Chlamydia* infection. Due to the often-asymptomatic nature of *Chlamydia* infection, the ultimate goal of *Chlamydia* research is to discover a vaccination against *Chlamydia* infection, which would be valuable in protecting individuals all over the world against the detrimental effects of *Chlamydia* infection.

CHAPTER 3

MATERIALS AND METHODS

Breeding of Mice, Infection with *Chlamydia*, and Collection of Vaginal Swabs

Male and female C57BL/6 mice carrying a Cre transgene under the urogenital epithelium-specific *Cdh16* promoter and Atg $5^{flox/flox}$ C57BL/6 mice were obtained. Animals were housed in a 12-hour light/dark cycle with food and water available *ad libitum*. All experimental protocols and procedures were completed in accordance with UMDNJ Animal Research Facility Guidelines.

A breeding schematic **(figure 2)** was followed in order to obtain mice with the genotype $Atg^{flox/flox}$, Epithelial Cre^{+} ($ECre^{+}$) for the experimental group, and mice with the genotype $Atg^{flox/flox}$, $ECre^{-}$ for the control group.

At the end of the breeding scheme, female mice, with each group including mice of experimental and control genotypes, were obtained. When the experimental and control female mice were between 5-7 weeks of age, two subcutaneous 2.5 mg medroxyprogesterone injections were administered within one week in order to sync the mouse menstrual cycles. The first medroxyprogesterone injection was administered seven days before *Chlamydia* infection, and the second medroxyprogesterone injection was administered three days before *Chlamydia* infection.

On day seven after the initial medroxyprogesterone injection, mice were infected with *Chlamydia*, 2×10^4 IFU of per 10µL/mouse, intravaginally **(figure 3)**. The *Chlamydia* was administered using fire-polished pipette tips in order to prevent

injury to the mice during infection. Each mouse was held in one hand by the tail and the scruff of the neck, with the anterior of the animal facing up. The *Chlamydia* solution was injected into the vagina of the mouse with a 20µl pipette. The mouse was then held in that position for several seconds before released back into its cage to prevent the *Chlamydia* from leaking out.

On day three after *Chlamydia* infection, vaginal swabs were acquired from each mouse and stored in 500µl of 2% BSA in SPG solution at – 80 C until day 70 after infection, when the swabs were thawed and used to estimate bacterial titers and the cytokine response to infection. Vaginal swabs were acquired again on day seven, and then once each week until eight swabs had been obtained **(figure 3)**. Each swab was obtained following the same protocol: the mouse was held in one hand by the tail and the scruff of the neck with its belly facing up. The swab was inserted into the vagina of the mouse and turned twenty times before it was removed and placed in the 2% BSA solution.

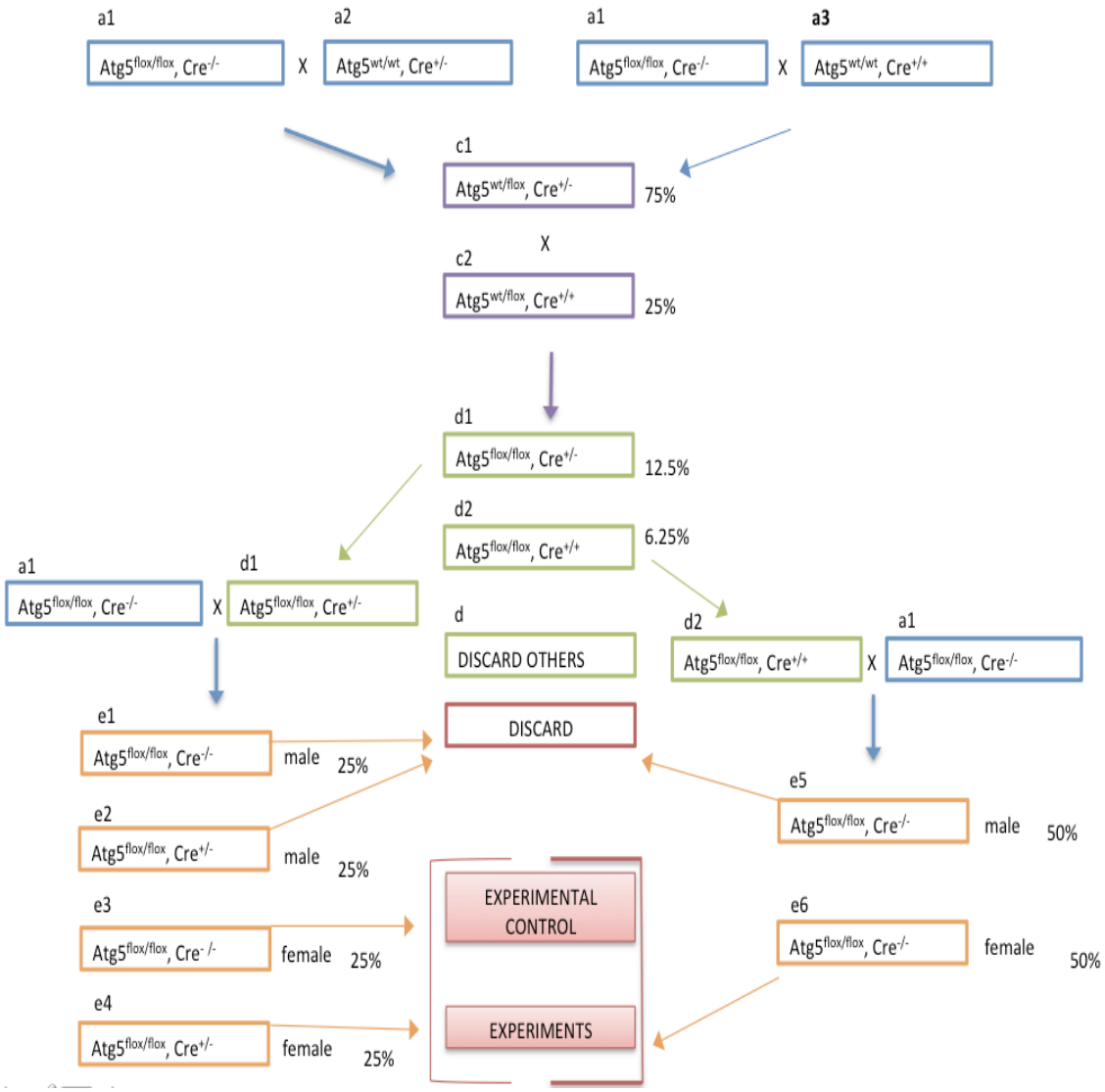

Figure 2. Mouse Breeding Scheme
Each box represents a mouse genotype. Percentages next to boxes indicate the probability of each genotype within a single litter.

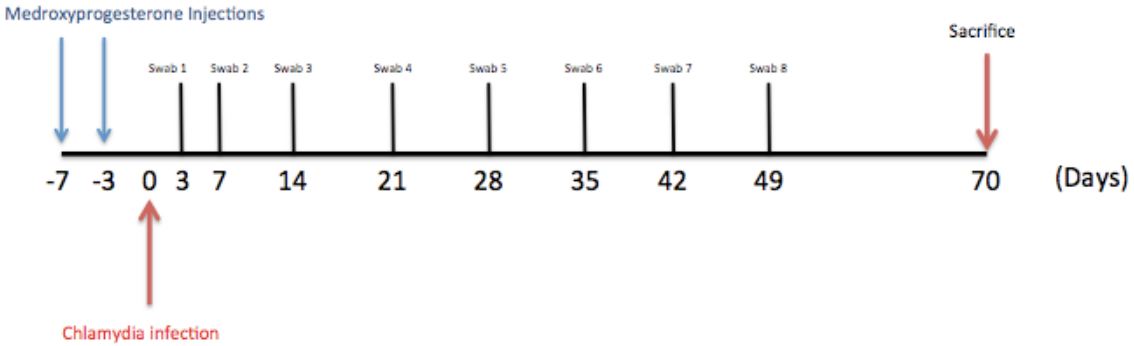

Figure 3. Model of *Chlamydia* infection and swabbing
Arrows represent days medroxyprogesterone injections were administered, mice were infected intravaginally with *Chlamydia*, and mice were harvested. Tick marks are labeled and represent days vaginal swabs were acquired.

Harvest of Tissues from Infected Animals

On day 70 after *Chlamydia* infection, mice were sacrificed by CO_2 inhalation followed by cervical dislocation. Immediately following sacrifice, the blood was harvested from the heart of each mouse using a 20-gauge needle and a syringe. The blood was then left to sit at room temperature for 3-4 hours before it was centrifuged at 1500 rpm. The serum was separated and stored.

Next, the spleens were removed from the mice and ground up using nylon mesh and the flat end of a 1.0 mL syringe. Splenocytes were washed and plated at 2×10^7 cells per well in a 24-well plate, with two wells for each spleen; one control well and one well for MoPn re-stimulation. In order to investigate the cytokines levels released by the splenocytes in response to *Chlamydia* in Epithelial Cre^+ mice as compared with Epithelial Cre^- mice, the splenocytes were re-stimulated with UV-inactivated MoPn at 0.5×10^6 IFU per well in 0.5mL of DMEM. SPG was used instead of MoPn in the control wells. The cells were incubated for 72 hours at 37°C and 5.5% CO_2. At 72 hours, the medium containing the cytokines that had been released by the splenocytes was removed from each well and stored at –80°C for ELISA assay after all groups of mice had been sacrificed..

Finally, the upper genital tracts of each sacrificed mouse were dissected and kept on ice for at least one hour, allowing the organs to become more firm and easier to handle. Dilation in the organs was recorded, and pictures were taken of each upper genital tract (UGT). The UGT was then submerged in formalin (10% formaldehyde) to fix overnight, washed three times with PBS, and stored at in 70% ethanol at 4^0C **(figure 7)**.

Quantification of EBs

In order to investigate the progression of *Chlamydia* infection in Epithelial Cre+ mice compared with control mice, vaginal swabs were taken every week throughout the course of the *Chlamydia* infection. The swabs were stored in 500µl 2% BSA in SPG solution at -80^{o}C for several weeks before bacterial titers were calculated.

To calculate *Chlamydia* titers, HeLa cells were plated and allowed to grow overnight to confluence on Fisherbrand microscope cover glass slides within the wells of a 24-well plate. The cells were then infected for 24 hours with *Chlamydia* from the bacteria swabs at a range of dilutions from 10^{0} to 10^{-7}.

After 24 hours of incubation at 37 ^{o}C and 5% CO_2, the infected cells were fixed with ice-cold methanol. The fixed cells were washed with PBS, and then incubated for 30 minutes using a primary mouse anti-*Chlamydia* muridarum (whole organism) antibody that had been collected from the serum of other *Chlamydia*-infected mice in our lab. After 30 minutes, the cells were again washed with PBS and incubated at room temperature with Anti-Mouse IgG (whole molecule)-FITC, produced in goat, which was purchased from Sigma. Following a final wash with PBS the immunostained coverslips were mounted on microscope slides. Inclusions were counted under an immunofluorescence microscope. Bacterial titers were calculated and recorded for each swab **(figure 5)**.

Determination of Intravaginal Cytokine levels

After the swabs were obtained from the mice, they were vortexed in 500 µl of 2% SPG in BSA and frozen at -80°C until all eight swabs had been collected. After the collection of the eighth swab, all swabs were thawed and used to assay cytokine levels at each point during the infection. TNF-α, IL-1α, and IL-6 cytokine levels were assayed by enzyme linked immunosorbant assay (ELISA) according to the protocol provided by the assay manufacturer. ELISA results were normalized to the standards provided by the manufacturer. TNF-α, IL-1α, and IL-6 data are presented as the amount of cytokine in pg per mL.

Determination of Splenocyte Cytokine response to *Chlamydia*

Media containing cytokines from the splenocytes challenged with MoPn or SPG over 72 hours were stored at -80°C prior to assay. Cytokines were released by splenocytes from $Atg^{flox/flox}$ Cre^{+} mice, and $Atg^{flox/flox}$ Cre- mice that were either re-stimulated with MoPn *Chlamydia* or SPG control. IL-4, IL-5, and IL-17 cytokine levels were assayed by enzyme linked immunosorbant assay (ELISA) according to the protocol provided by the assay manufacturer. ELISA results were normalized to the standards provided by the manufacturer. IL-4, IL-5, and IL-17 data are presented as the amount of cytokine in pg per mL.

Statistical analysis

Two-sided T test was performed on Microsoft Excel to analyze the EB titers and cytokine data. Two-sided Fisher Exact test was performed to analyze the pathology data. A significant difference was defined as p-value of <0.05.

P62-deficient Animal Experiments

In order to further explore the pathology of *Chlamydia* infection in relation to autophagy machinery, we decided to perform the above experiments on a second cohort of animals. Two p62-deficient animals were obtained; one male and one female. These two animals were bred together, resulting in five female p62-deficient offspring.

Five wild type control female B6 mice were obtained as counterparts to the five female p62 mice. The control animals were the same age as the p62-deficent animals, and they were housed under the same conditions as p62 animals in a separate cage to prevent over-crowding.

When the mice were six weeks of age they were infected with *Chlamydia* as detailed above. Vaginal swabs were obtained and stored following the same protocol as for the epithelial Cre animal cohort. Bacterial titrations were estimated from each swab using the immunostaining protocol, and on day 50 after infection the mice were sacrificed.

The upper genital tracts of all animals were dissected and photographed under the same conditions as the Epithelial Cre cohort of animals to explore the physiopathology of the infection in the two groups of animals.

ELISA assay was performed on the first four swabs to investigate TNF-α, IL-1α, and IL-6 cytokine response. As detailed above, ELISA results were normalized to the standards provided by the manufacturer.

CHAPTER 4

RESULTS

Breeding Mice to Develop ATG5 Knock Out

We first developed ATG5 Knockout mice using the Cre/Lox system by following the breeding scheme pictured in **figure 2**. Four final litters of mice were obtained from this breeding. The females were separated from the males in each litter and they were genotyped using CRE and ATG PCR. Litter 1 included one Cre+ ATG5 knockout female mouse, and two Cre- wild-type female mice. Litters 2 and 4 included two each of Cre + ATG5 knockout and Cre- wild-type female mice. Litter 3 included three Cre + ATG5 knockout female mice and four Cre – wild-type female mice. Experimental (ATG5 knockout) mice and Control (WT) mice of the same litter were housed together in the same cage to minimize any confounding factors having to do with their feeding and care throughout the experiment. An example of Cre and ATG5 genotyping is pictured in **figure 4**.

Overall, the breeding process resulted in a total of 18 female animals: 10 Cre-$Atg^{flox/flox}$ control animals, and 8 Cre+$Atg^{flox/flox}$ experimental animals.

A.

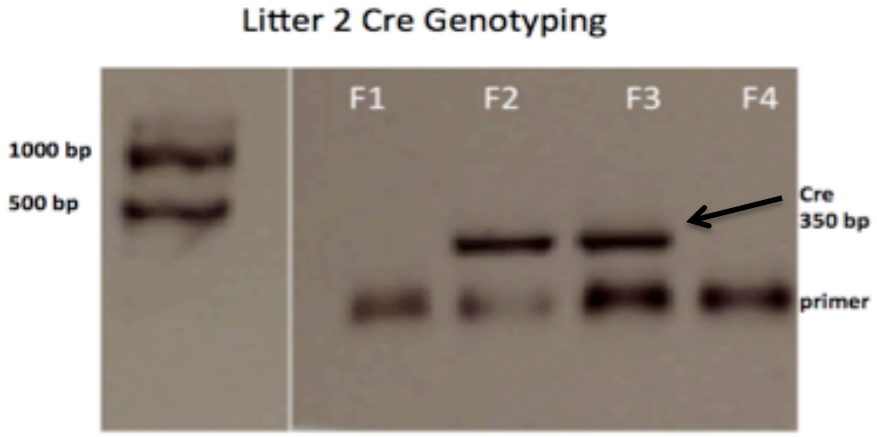

B.

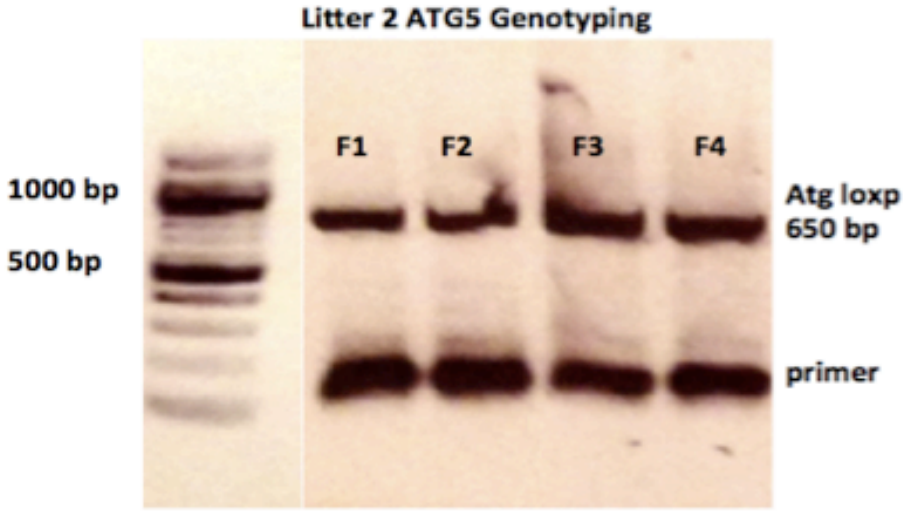

Figure 4. Litter 2 Cre and ATG5 Genotyping
An example of Cre and ATG5 genotyping. Panel A is an agarose gel with DNA loaded from Cre + PCR. The Cre + band is marked with an arrow at 350 bp. The 100 bp ladder is pictured to the left of the gel. Panel B is an agarose gel with DNA loaded from ATG5 PCR. The Atg loxp band is at 650 bp, as shown by the 100 bp ladder to the left of the gel image. In this litter, all animals are $Atg^{flox/flox}$ genotype. Animals F2 and F3 are Cre+ genotype, and therefore they are ATG5 knockout animals. Animals F1 and F4 are the control group for this litter.

Bacterial Titers

Following intravaginal *Chlamydia* infection of the mice, swabs were taken once per week at time points indicated in **figure 3**, and the swabs were stored at -80°C in 500µl of 2% BSA in SPG solution. Swabs were thawed and the bacterial titers were calculated via serially infected HeLa cells that were immunostained for *Chlamydia* inclusions. Immunostained inclusions glow green under the fluorescent microscope.

The two-sided T test between Cre + experimental group and Cre – Control group for each swab demonstrated no significant difference in the bacterial titers. For each animal, the *Chlamydia* titer was highest 3 days after infection and decreased every week after that as the infection was cleared **(figure 5)**.

On day three, swab 1, the average bacterial titer for the Cre + $Atg^{flox/flox}$ animals was 5.9×10^4 ifu/mL, and similarly the average bacterial titer for the Cre – $Atg^{flox/flox}$ animals was 5.7×10^4 ifu/mL. Immunostaining of the remaining swabs displayed a gradual decrease in bacterial titer for both the experimental and control groups of animals. The Cre + $Atg^{flox/flox}$ experimental animals had average bacterial titers of swab 2: 1.7×10^4 ifu/mL, swab 3: 1.5×10^3 ifu/mL, swab 4: 1.1×10^3 ifu/mL, swab 5: 3.9×10^2 ifu/mL, swab 6: 17 ifu/mL, and swabs 7 and 8 were 0 ifu/mL. The Cre – $Atg^{flox/flox}$ control animals displayed bacterial titers of swab 2: 2.8×10^3 ifu/mL, swab 3: 1.2×10^3 ifu/mL, swab 4: 4.7×10^2 ifu/mL, swab 5: 18.4 ifu/mL, and swabs 7 and 8 were 0 ifu/mL. The experimental mice deficient in autophagy displayed the same ability to clear bacterial load as their wild-type counterparts, as demonstrated by the graph in **figure 5**. A two-sided T-test was performed between the epithelial

autophagy-deficient animals and the epithelial autophagy-proficient animals for each swab. While a p-value of <.05 would have been considered a significant difference in bacterial titer between the two groups, the p-values for each of the swabs ranged from .24 - .48 **(figure 5)**.

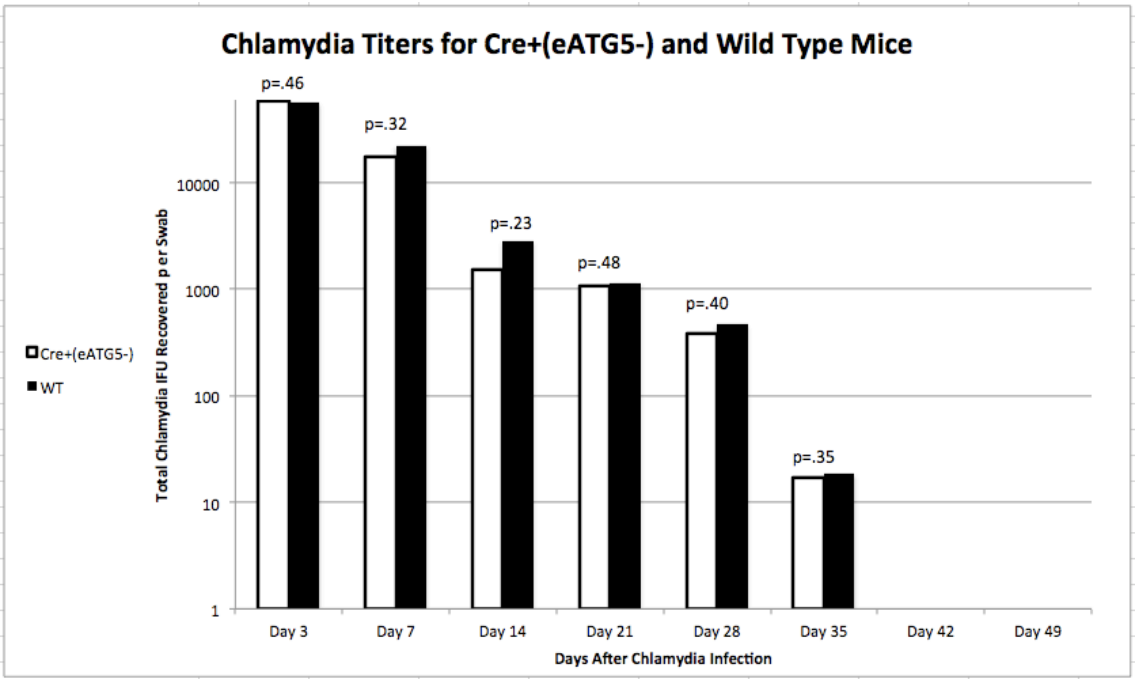

Figure 5. *Chlamydia* Titers for Cre+(ATG5-) and Cre–(Wild Type) Mice. This figure quantifies the *Chlamydia* titers for cre+(eATG5-) mice in white and cre-(WT) mice in black. The number of *Chlamydia* IFUs recovered per swab is represented the Y-axis. The highest average bacterial titer was day three, 5.9 x 10^4 ifu/mL in cre+(eATG5-) mice, and similarly Day 3 WT titer was 5.7 x 10^4 ifu/mL. By day 42 after infection, the bacterial load was reduced to zero. Cre+(ATG5-) vs. cre-(WT) P values are included for each bacterial titer. The *Chlamydia* titers were statistically the same in cre+(ATG5-) mice and cre-(WT) mice at every point during *Chlamydia* infection.

Pathology of the Infection

70 days after intravaginal *Chlamydia* infection, animals were sacrificed by CO_2 inhalation and cervical dislocation, and their upper genital tracts were removed for observation. Unilateral hydrosalpinx were found in two of the ten Cre+Atg$^{flox/flox}$ animals, and three of the eight Cre-Atg$^{flox/flox}$ control animals. Bilateral hydrosalpinx were found in one of the ten Cre+Atg$^{flox/flox}$ experimental mice **(figure 6)**. The hydrosalpinx were observed to be bubble-like swellings on the ovaries of the animals that sometimes curled around to look like the shell of a snail. The hydrosalpinx were very delicate and prone to breaking during the process of dissection.

The remaining animals displayed no hydrosalpinx. A two-sided Fisher's exact test revealed no significant difference in pathophysiology between the infected autophagy-deficient and infected autophagy-proficient animals. The urogenital tracts and ovaries of all infected mice are displayed in **figure 7**. The differences in size and shape between the urogenital tracts in the pictures are representative of expected phenotypic variance between animals, and they are not the result of *Chlamydia* infection.

Instance of Hydrosalpinx in ATG5- and Wild Type Mice			
	Unilateral Hydrosalpinx	Bilateral Hydrosalpinx	No Hydrosalpinx
Cre + (eAtg5-/-)	2	1	5
Cre - (WT)	3	0	7
ATG5- v. WT p-value	1	1	1

Figure 6. Instance of Hydrosalpinx in Cre+(eATG5-) and Wild Type Mice
Quantification of pathology data from Autophagy-deficient Cre+Atg$^{flox/flox}$ and WT Cre-Atg$^{flox/flox}$ *Chlamydia*-infected mice. The Fisher exact test results between Cre+ and Cre- animals of each phenotype are included.

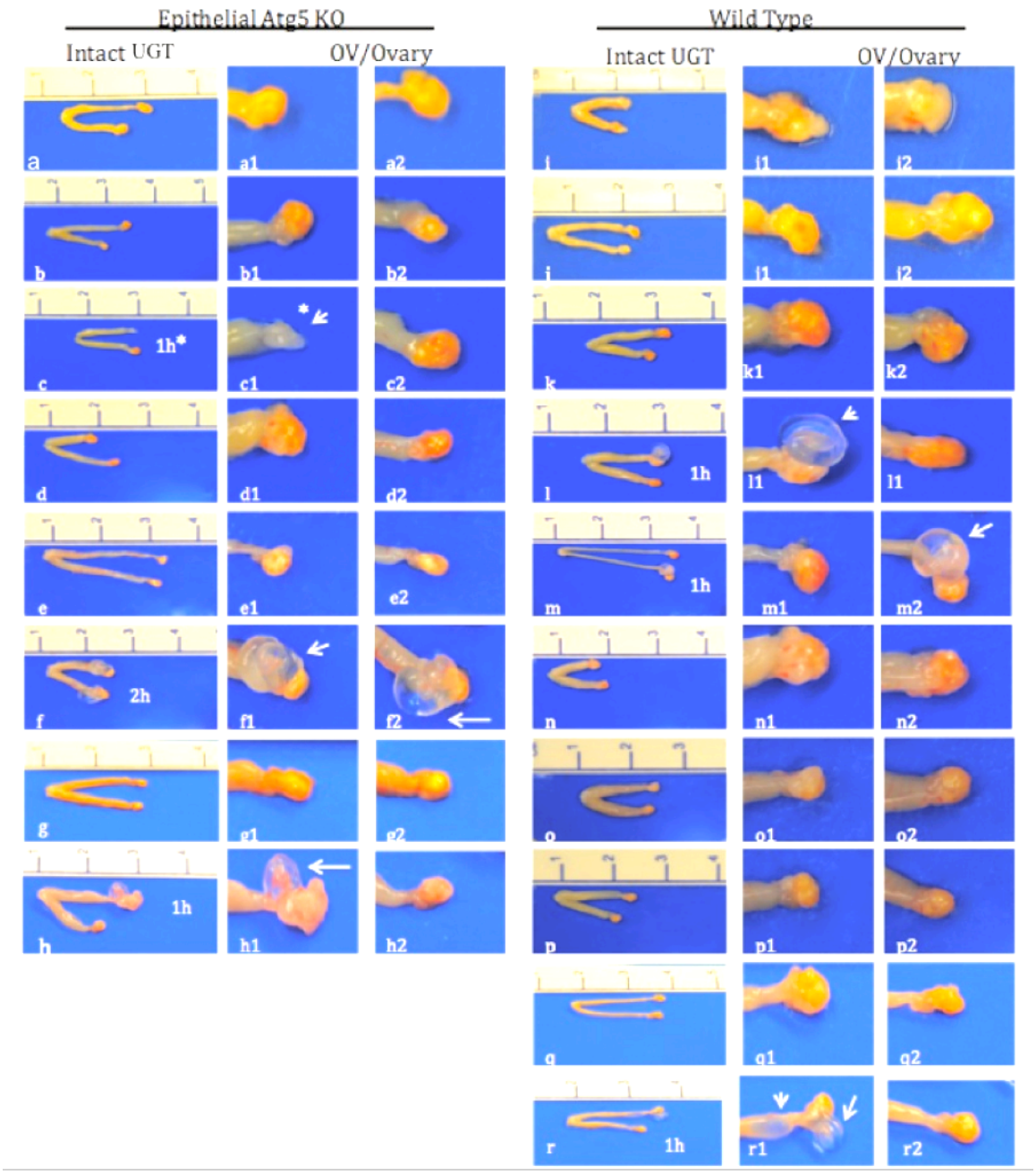

Figure 7. Pathology of *Chlamydia* infection
Epithelial Atg5 KO UGT are pictured on the left and WT UGT are pictured on the right. "1h" or "2h" is noted if the UGT had one or two hydrosalpinx. Ovaries are magnified beside each UGT. Arrows indicate dilation and hydrosalpinx in the magnified pictures.

Splenocyte Cytokine Response

After all of the vaginal swabs were collected, we chose to conduct an ELISA assay in order to investigate cytokine expression as the mice fought off the *Chlamydia* infection. The spleens were collected from each animal and splenocytes were plated and restimulated with MoPn or SPG as a control. There was no apparent difference in the size and shape of the spleens of experimental and control animals, although no specific data was taken with regards to the mass of the spleens. The cells were given 72 hours to react to the restimulation with UV-irradiated UVs before the cytokine-containing media was collected for ELISA assay.

The splenocyte samples were assayed for IL-4, IL-5, and IL-17 (**figures 8, 9, 10**). For each of the cytokines assayed, a two-sided T Test confirmed a marked increase in cytokine response after splenocytes were restimulated with murine *Chlamydia* MoPn as compared with the controls.

Another two-sided T test revealed that there was no significant difference in cytokine response between the splenocytes of autophagy-deficient Cre+$Atg^{flox/flox}$ animals and the splenocytes of autophagy-proficient Cre–$Atg^{flox/flox}$ animals. The statistical analysis and cytokine levels presented in graph-form can be found in **figures 8, 9, and 10.**

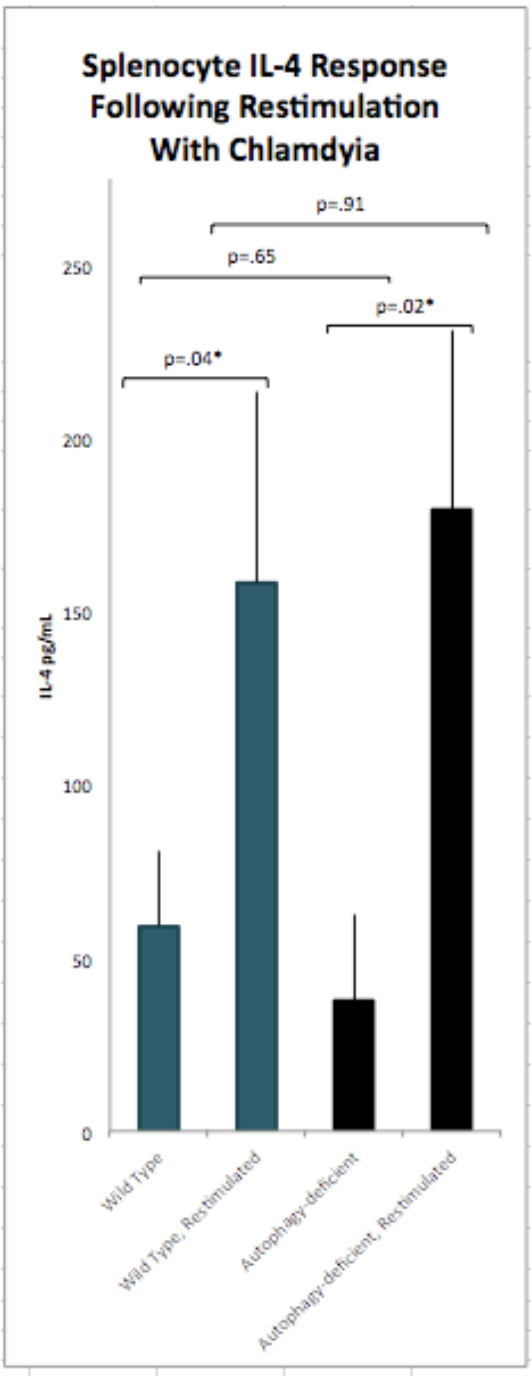

Figure 8. Splenocyte IL-4 Cytokine Response after Restimulation.
The Y-axis represents cytokine concentration from 0-250 pg/mL. Black bars demonstrate standard deviation within each group of animals. P-values are displayed, and one asterisk indicates P<.05.

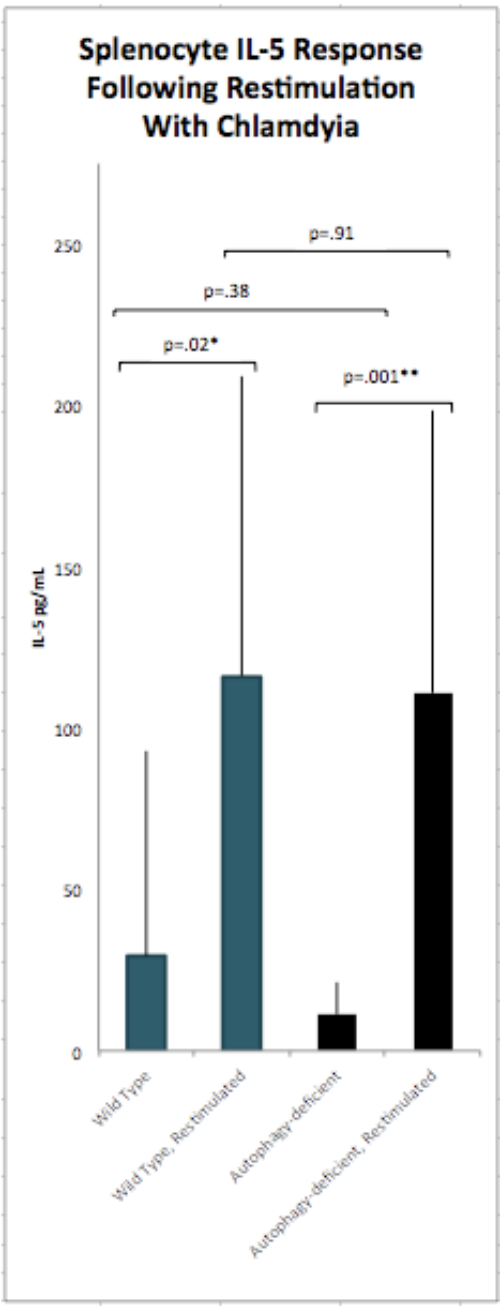

Figure 9. Splenocyte IL-5 Cytokine Response after Restimulation.
The Y-axis represents cytokine concentration from 0-250 pg/mL. Black bars demonstrate standard deviation within each group of animals. P-values are displayed and one or two asterisks mark $P<0.05$ and $P<0.01$, respectively.

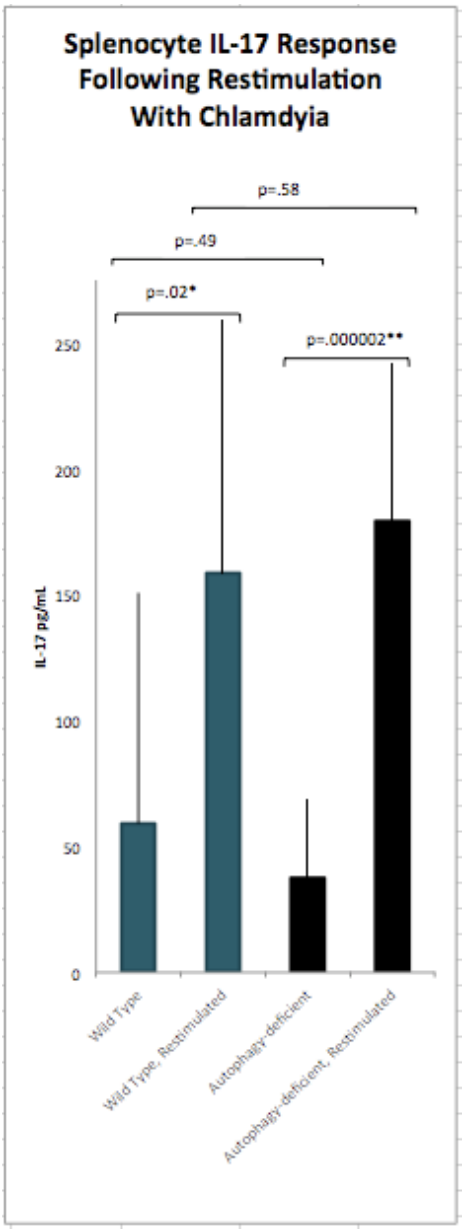

Figure 10. Splenocyte IL-17 Cytokine Response after Restimulation.
The Y-axis represents cytokine concentration from 0-250 pg/mL. Black bars demonstrate standard deviation within each group of animals. P-values are displayed and one or two asterisks mark $P<0.05$ and $P<0.01$, respectively.

Intravaginal Cytokine Response

Swabs were acquired from all infected mice three days after intravaginal *Chlamydia* infection, seven days after infection, and then once each week after the initial swabs. During the collection of swabs, there was no noticeable difference between the experimental and control groups of animals with regards to vaginal swelling. The control and experimental animals had no apparent difference in size, weight, or physical activity. Due to being housed in the same cages, experimental and control animals experienced the same environmental factors throughout *Chlamydia* infection. Following collection, the swabs were placed in 500µl of 2% BSA in SPG solution and vortexed prior to freezing at -80^{o}C.

Cytokine assays for IL-1, IL-6, and TNF-α were performed on all swabs.

The data suggests that on day three after infection, initial cytokine response is relatively low for all three cytokines in autophagy-deficient and autophagy-proficient animals. By day 7 after initial infection (swab 2), in all instances the cytokine response had increased, indicating that by this time the mouse immune response to the infection was underway. The IL-1α response in experimental animals and the TNFα cytokine response in control animals increased slightly after day 7, while all other cases the cytokine response began to decrease after day 7 of the infection.

Two weeks after infection, the cytokine response gradually decreased, mirroring the decreasing bacterial load. The infection was cleared by weeks six and seven (swabs

seven and eight) at which point cytokine expression was very low **(figures 11, 12, 13)**.

Each of the cytokine assays for IL-1, IL-6, and TNF-α revealed no statistical difference in cytokine response between Cre+ $Atg^{flox/flox}$ autophagy-deficient mice and Cre-$Atg^{flox/flox}$ autophagy-proficient mice, as shown by the T Tests displayed in **figures 11, 12, and 13**, respectively.

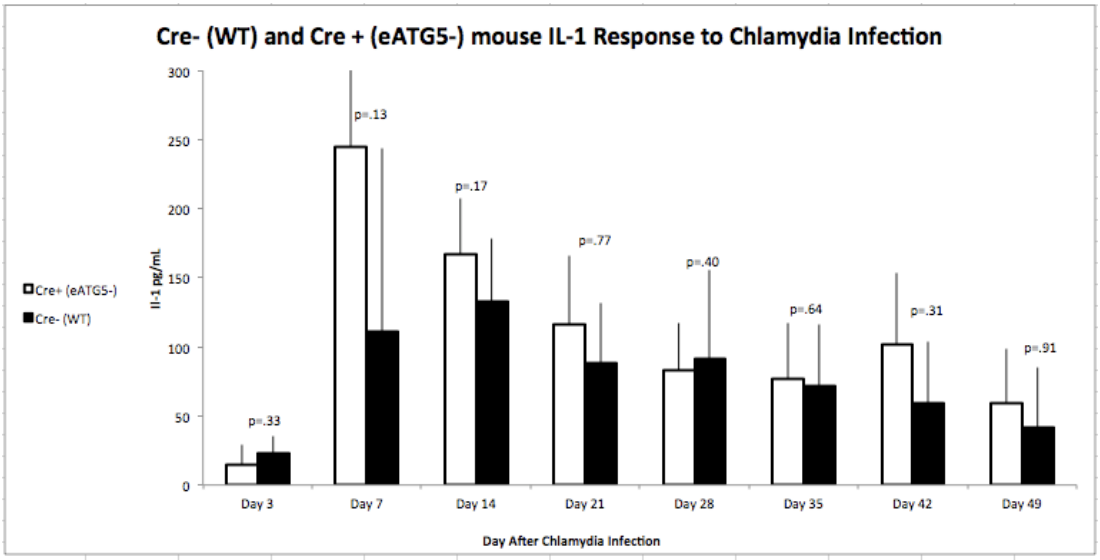

Figure 11. IL-1 Response Throughout *Chlamydia* Infection
Represents the Cre+(eATG5-) and Cre-(WT) IL-1α response to *Chlamydia* infection on days 3-49 after infection. IL-1 concentration is displayed on the Y-axis in pg/mL. P-values from a Cre+(eATG5-) vs. Cre-(WT) T Test are included.

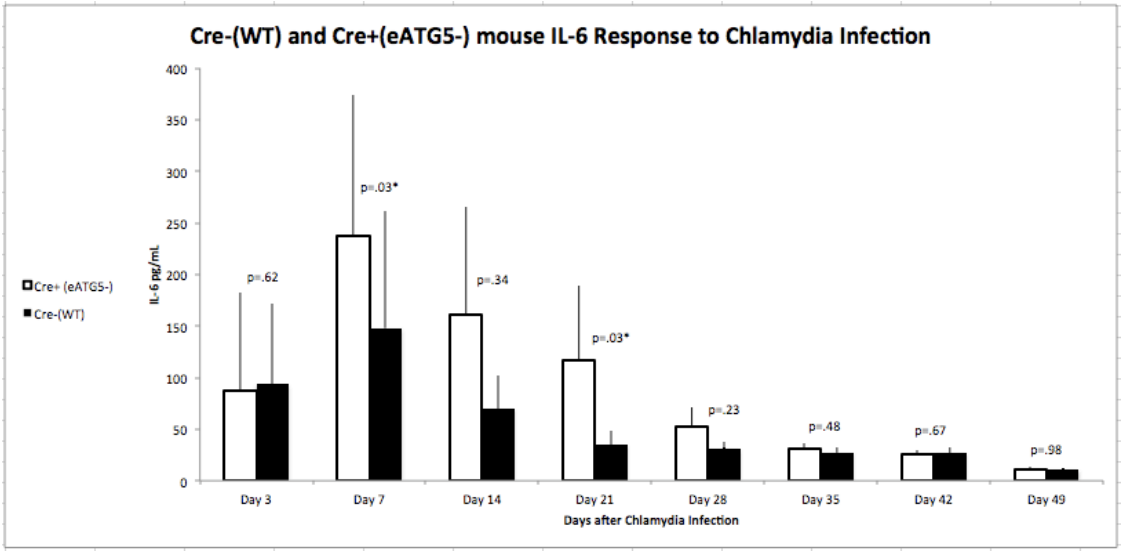

Figure 12. IL-6 Response Throughout *Chlamydia* Infection
Cre+(eATG5-) and Cre-(WT) IL-6 response to *Chlamydia* infection on days 3-49 after infection. IL-6 concentration is displayed on the Y-axis in pg/mL. P-values representing the statistical difference between the cytokine response in Cre+(eATG5-) vs. Cre-(WT) on each day are included.

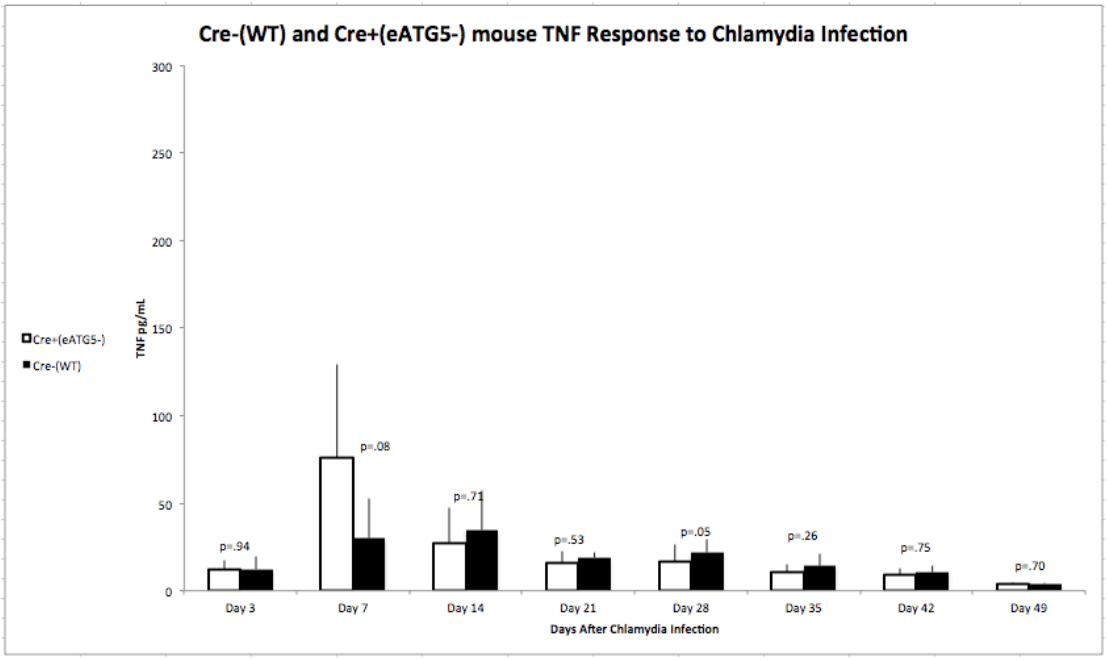

Figure 13. TNFα Response Throughout *Chlamydia* Infection
Cre+(eATG5-) and Cre-(WT) TNFα response to *Chlamydia* infection on days 3-49 after infection. TNFα concentration is displayed on the Y-axis in pg/mL. P-values from a Cre+(eATG5-) vs. Cre-(WT) T Test are included.

P62-Deficient Cohort Results

Five female p62-deficient mice and five female wild type mice were intravaginally infected with *Chlamydia* at six weeks of age using the same infection protocol we had previously used on epithelial autophagy-deficient animals. It was observed that the p62-deficient animals gained more weight than the wild type animals. Both groups of animals had the same access to food and water, leading us to believe that the phenotypic difference may be a result of the lack of p62 in the p62-deficient animals.

Chlamydia titers were counted using immunostaining and a fluorescent microscope. For both p62-deficient and wild type groups of animals, the highest bacterial count was swab 1, which was taken three days after the mice were infected with *Chlamydia*. The *Chlamydia* titer gradually decreased in all animals until week 6 after infection, when the infection was completely cleared. A two-sided T Test was performed between the *Chlamydia* titer count of p62-deficient group and the wild type group of *Chlamydia*-infected animals. A T Test result of $p < .05$ is considered a significant difference, and we discovered no significant difference between the two groups of animals at any point during infection **(figure 16)**.

On day 60 after infection, the mice were sacrificed and their upper genital tracts were removed for observation **(figure 15)**. Of the five wild type *Chlamydia*-infected mice, three displayed unilateral hydrosalpinx. Similarly, of the five p62-deficient *Chlamydia*-infected animals, two displayed unilateral hydrosalpinx and one displayed severe dilation of the upper genital tract. Based on these results, a two-sided Fisher Exact test revealed that there was no significant difference in

pathophysiology of the upper genital tracts between wild type and p62-deficient *Chlamydia*-infected mice.

An ELISA assay was performed on swabs 1-4 to examine the expression of cytokines IL-1α, IL-6, and TNFα. In both wild type and p62-deficient groups of *Chlamydia*-infected animals, cytokine expression was highest in swab 2, which was taken one week after intravaginal *Chlamydia* infection. IL-1α, IL-6, and TNFα expression decreased following the first week of *Chlamydia* infection. Statistical analysis comparing the cytokine response in p62-deficient animals compared to wild type animals revealed no significant difference for any of the cytokines tested **(figures 17, 18, 19)**.

Instance of Hydrosalpinx in p62 and Wild Type Mice			
	Unilateral Hydrosalpinx	Bilateral Hydrosalpinx	No Hydrosalpinx
p62-Deficient	2	1	2
Wild Type	3	0	2
p62 v. WT p-value	1	1	1

Figure 14. Instance of Hydrosalpinx in p62-deficient and Wild Type Mice
A quantification of the pathology data from Cre+Atg$^{flox/flox}$ and WT Cre-Atg$^{flox/flox}$ *Chlamydia*-infected mice. The number of mice that displayed each pathology of the infection is indicated on the Y-axis. Results from two-sided Fisher Exact tests for Cre+ vs. Cre- mice of each phenotype are included.

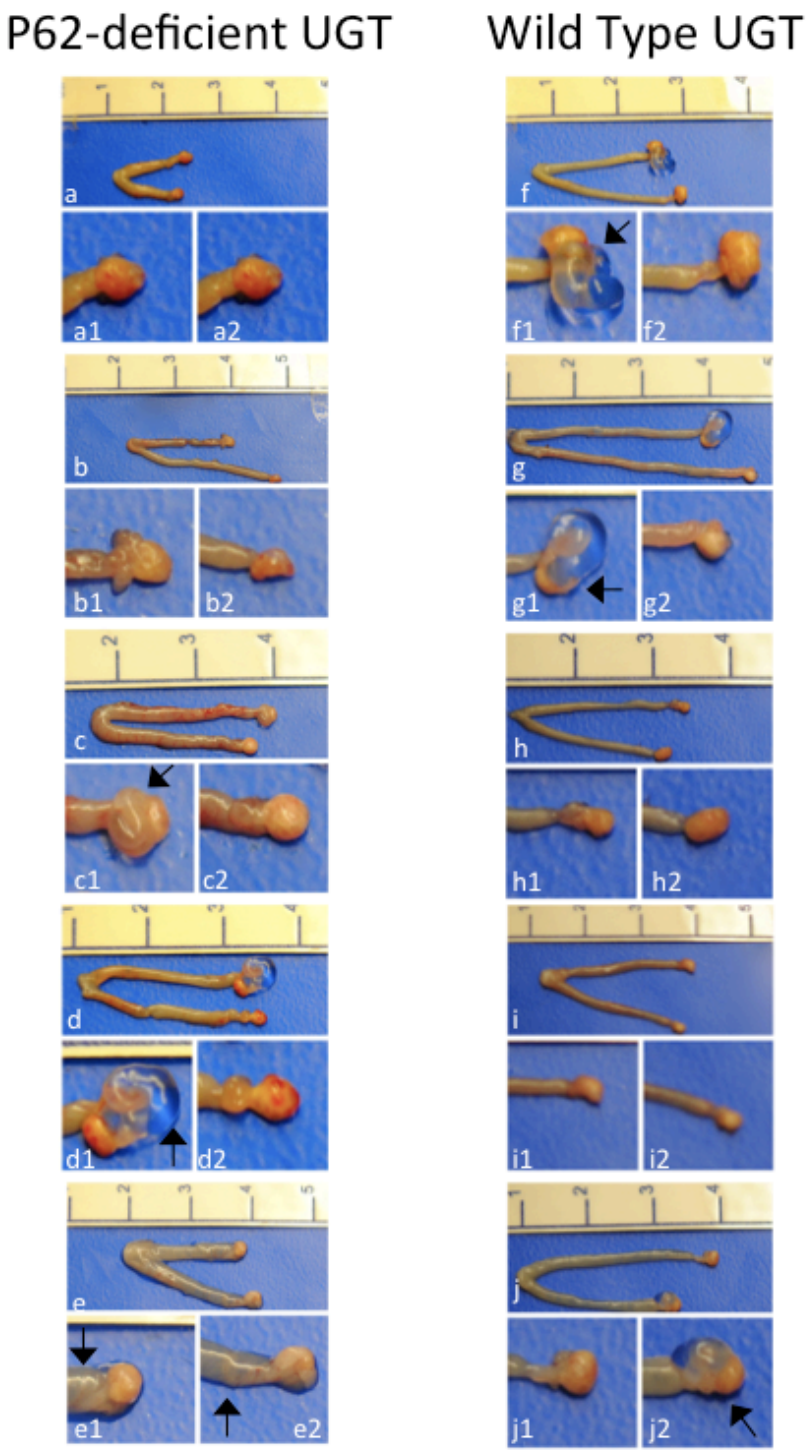

Figure 15. Pathology of *Chlamydia* infection in P62 Cohort
P62-deficient UGT are pictured on the left, while WT UGT are pictured on the right. Ovaries are magnified below each UGT. Arrows indicate dilation and hydrosalpinx in the magnified pictures.

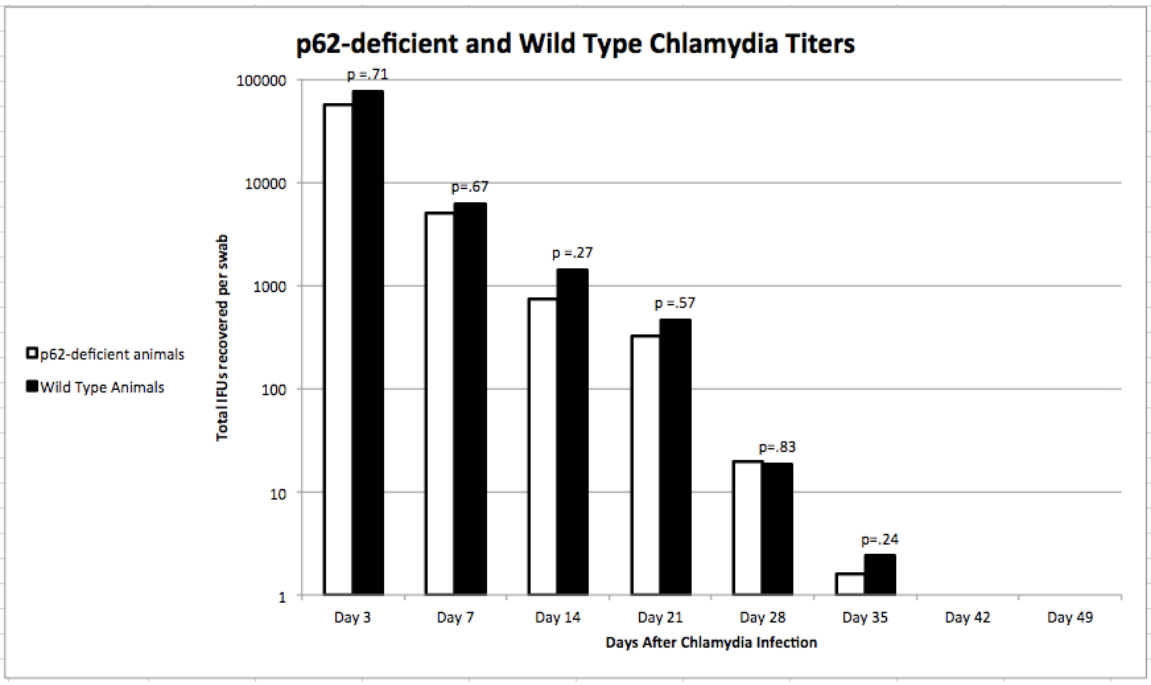

Figure 16. *Chlamydia* Titers released from swabs for p62-deficient and Wild Type Mice

This figure quantifies the *Chlamydia* titers for p62-deficient mice in white and WT mice in black. The number of *Chlamydia* IFUs recovered per swab is represented the Y-axis. The highest number of inclusions was recorded on day 3 after *Chlamydia* infection for both groups of mice. By day 42 after infection, the bacterial load was reduced to zero. The p values from a P62-deficient *Chlamydia* titer vs. WT *Chlamydia* titer two-sided T Test are included for each bacterial titer. The *Chlamydia* titers were statistically the same in p62-deficient mice and WT mice at every point during *Chlamydia* infection.

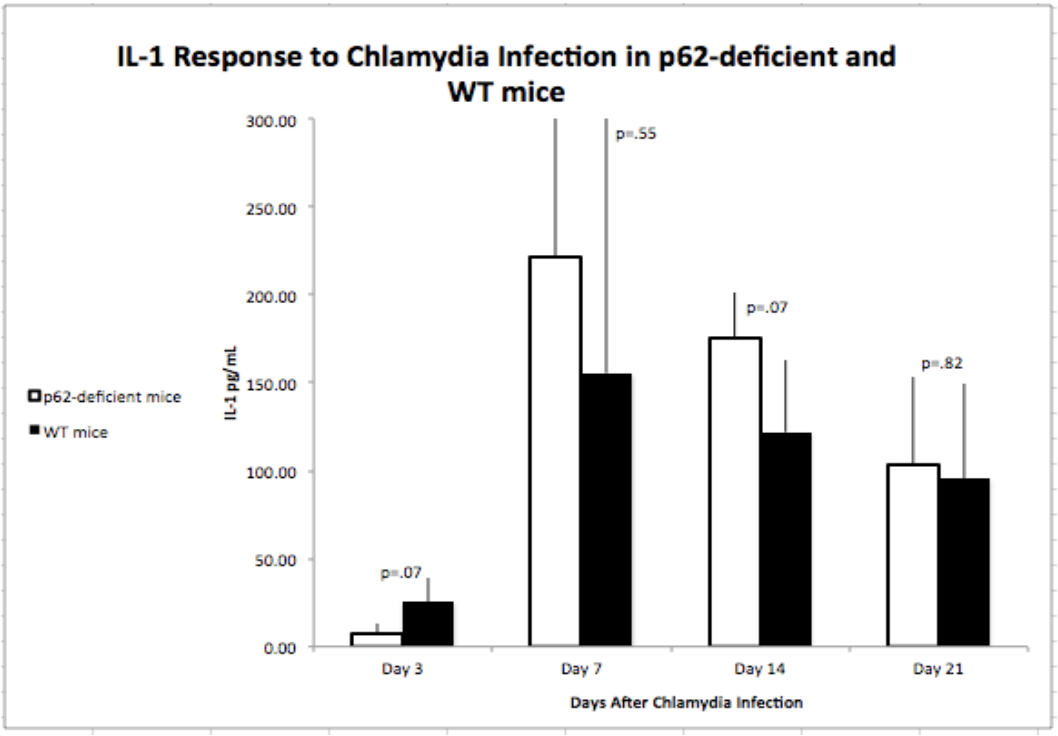

Figure 17. IL-1 Response after *Chlamydia* Infection in p62 Cohort
P62 and WT groups IL-1α response to *Chlamydia* infection on days 3-49 after infection. IL-1 concentration is displayed on the Y-axis in pg/mL. P-values representing the statistical difference between the cytokine responses in p62 vs. WT mice on each day are included.

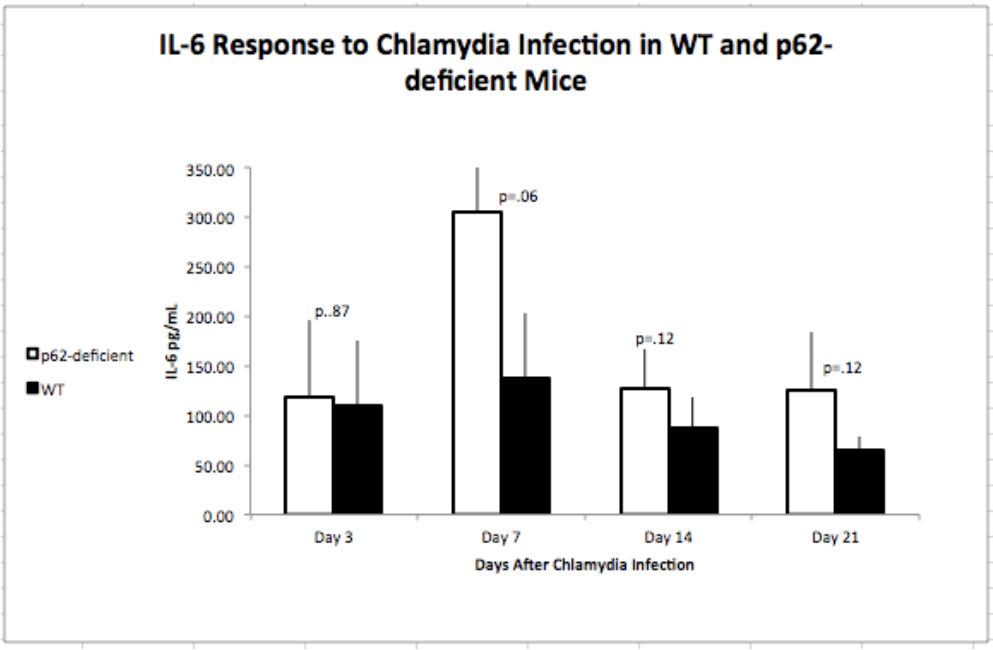

Figure 18. IL-6 Response after *Chlamydia* Infection in P62 Cohort
P62 and WT groups IL-6 response to *Chlamydia* infection on days 3-49 after infection. IL-6 concentration is displayed on the Y-axis in pg/mL. P-values representing the statistical difference between the cytokine responses in p62 vs. WT mice on each day are included.

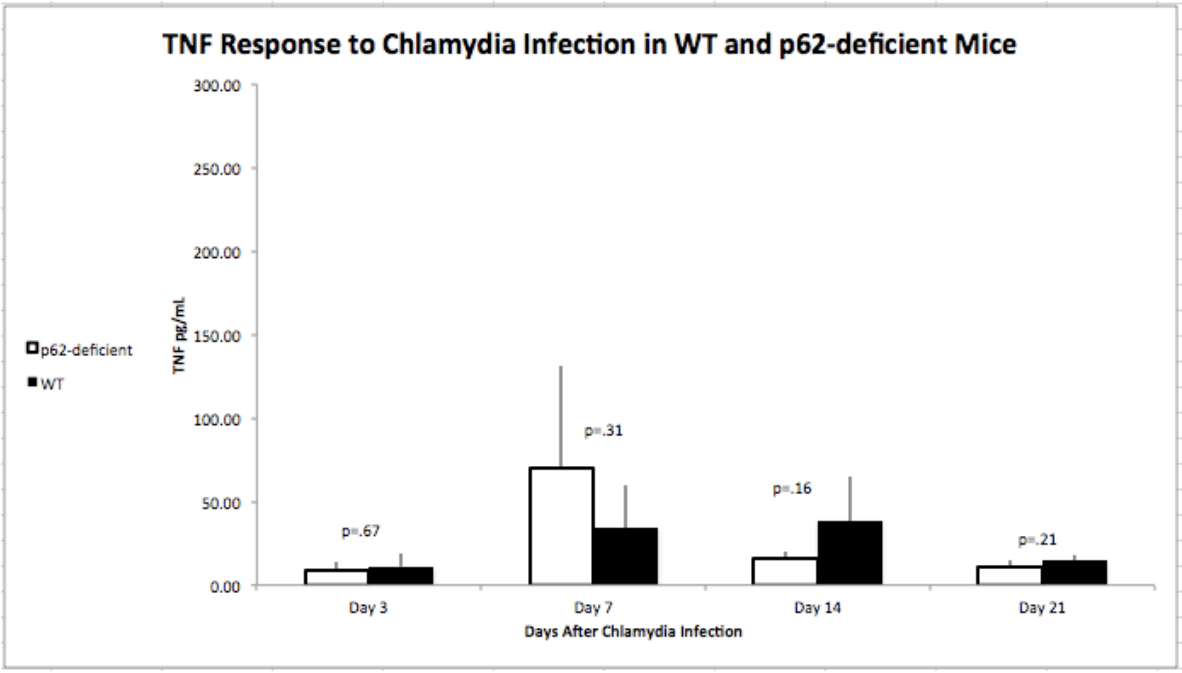

Figure 19. TNFα Response after *Chlamydia* Infection in P62 Cohort
P62 and WT groups TNFα response to *Chlamydia* infection on days 3-49 after infection. TNFα concentration is displayed on the Y-axis in pg/mL. P-values representing the statistical difference between the cytokine responses in p62 vs. WT mice on each day are included.

CHAPTER 5

SUMMARY AND DISCUSSION

Worldwide, *Chlamydia* is the most common sexually transmitted bacterial infection [3]. *Chlamydia* is particularly dangerous because it is often symptomless, and therefore despite serious long-term complications of the infection, many infected patients go untreated allowing the infection to progress and be transmitted to more people [3]. Following initial *Chlamydia* infection, the infection in women ascends to the upper genital tract causing the formation of hydrosalpinx, or inflammation of the ovaries [3]. Ascension of the infection to the upper genital tract results in complications including pelvic inflammatory disease and infertility. Despite the seriousness and prevalence of *Chlamydia*, the molecular pathology of the disease as it ascends to the upper genital tract has not been completely elucidated. This study seeks to investigate the molecular pathology of *Chlamydia*.

In addition to a lack of clarity surrounding the pathology of *Chlamydia* infection, reports of the interaction between host autophagy and *Chlamydia* infection paint a complicated picture [11]. To begin, *Chlamydia* triggers an autophagy response. Previous studies have found that *Chlamydia* infection leads to increase in markers for autophagy while the rate of long-lived protein degradation (LLPD) remains constant or decreased [24]. This data alone suggests an immune response to the *Chlamydia* infection via the autophagy pathway. However, the nature of the autophagy response to *Chlamydia* is not so straightforward. Other studies

demonstrated that the *Chlamydia* inclusion does not fuse with the lysosome in epithelial cells [11-16], which are known to be the primary target of *Chlamydia* [11, 28, 29]. Our lab previously reported that ATG5 gene knockout-induced autophagy deficiency had no effect on L2 growth in embryonic fibroblasts (MEFs)[24]. *Chlamydia* EBs are degraded in the lysosomes of other cells, including blood monocytes and neutrophils [17-19]. This data suggests that *Chlamydia* may have evolved a mechanism to evade host autophagy in epithelial cells, promoting further infection and species survival. Yet, the picture of *Chlamydia* infection is still not complete. Another study demonstrated that autophagy deficiency due to ATG5-knockout in myeloid cells of mice resulted in a significantly more severe upper genital tract pathology following *Chlamydia* infection than the pathology in mice that were proficient in autophagy (unpublished). This data underscores the importance of autophagy as a host response for fighting off invading EBs in granulocytes and macrophages.

The current study attempts to assess epithelial autophagy in *Chlamydia* infection in vivo, in order to add to the broad picture of the role of autophagy in *Chlamydia* infection that has been investigated in previous studies in vitro. The autophagy gene ATG5 was knocked out in epithelial cells of mice, resulting in animals that were autophagy deficient in genital epithelial cells, the primary target of *Chlamydia* bacteria [11, 28, 29]. The mouse pathogen *C. muridarum* (MoPn) was found to be a useful species in this study because it models human *Chlamydia* infection in mice [25, 40, 41]. ATG5-knockout animals and WT animals were infected with *C. muridarum* and the infection was monitored to investigate the effect of autophagy-

deficiency on *Chlamydia* infection in mice. This study was considered a logical next step in studying *Chlamydia* infection because a significant difference in physiopathology between Cre+Atg$^{flox/flox}$ autophagy-deficient animals and Cre-Atg$^{flox/flox}$ autophagy-proficient animals would challenge the hypothesis that *Chlamydia* evades epithelial autophagy. However, if the *Chlamydia* infection resulted in similar pathology between the two experimental groups of animals, these results would support the previous hypothesis that *Chlamydia* bacteria exert a survival mechanism that allows them to evade epithelial autophagy.

Following *Chlamydia* infection, the *Chlamydia* bacterial titers were immunostained and counted. *Chlamydia* titers in both the wild-type group and the autophagy-deficient group of animals gradually decreased over the course of 6 weeks, until the infection was cleared. The rate of bacterial clearance was similar between both epithelial autophagy-deficient animals and wild-type animals, and a two-sided T-test revealed no significant difference between the two groups of mice. These data are consistent with the hypothesis that *Chlamydia* evades host epithelial autophagy; knocking out host epithelial autophagy does not result in increased *Chlamydia* survival. The bacterial titer results in the current study support the data from previous studies in which autophagy machinery was found to be triggered as an immune response to *Chlamydia* only in non-epithelial cells, despite the fact that epithelial cells are the primary target of *Chlamydia* [11, 28, 29].

After the animals were infected with *Chlamydia* and the infection cleared, the mice were sacrificed and the upper genital tract of each mouse was removed for observation **(figure 7)**. The pathophysiology results were consistent with the

hypothesis that *Chlamydia* evade epithelial cell autophagy. There was swelling and hydrosalpinx in some of the animal upper genital tracts, and others were without hydrosalpinx. Overall, two-sided Fisher exact tests between the Cre+$Atg^{flox/flox}$ epithelial autophagy-deficient animals and the Cre – $Atg^{flox/flox}$ epithelial autophagy-proficient animals revealed no significant difference in the pathophysiology between the groups. As mentioned above, host autophagy machinery is usually triggered as an immune response to *Chlamydia* infection, and therefore one would expect that knocking out autophagy in the primary target of *Chlamydia* would result in impaired ability of autophagy knockout mice to fight *Chlamydia* infection. The hypothesis that *Chlamydia* evades or down-regulates host autophagy in wild type animals is supported by the similarity in pathophysiology between infected wild type animals and infected epithelial autophagy knockout animals in the current study.

Cytokine analysis was performed on the restimulated splenocytes from the animals and on all of the vaginal swabs that were taken from the mice throughout *Chlamydia* infection. Overall, two-sided T test between the epithelial autophagy-deficient animal cytokines and the autophagy proficient animal cytokines revealed no significant difference between the cytokine response of the two groups throughout the course of the infection and after splenocyte restimulation with MoPn. Both the autophagy-deficient experimental animals and autophagy-proficient control animals experienced a significant increase in IL-4, IL-5, and IL-17 cytokine production following splenocyte restimulation with MoPn in vitro as compared with un-stimulated control splenocytes. The cytokine expression is expected to be

upregulated following restimulation in order to help facilitate an immune response to *Chlamydia* infection. However, the ability of the splenocytes to respond to restimulation was consistent between the autophagy-deficient experimental animals and the autophagy-proficient control animals.

The cytokine results from vaginal swabs taken throughout the course of *Chlamydia* infection revealed an increase in cytokine production in the second week of the infection, and then cytokine levels gradually decreased as the infection was cleared. However, the cytokine levels throughout infection were not statistically different between Cre+Atg$^{flox/flox}$ epithelial autophagy-deficient animals and Cre-Atg$^{flox/flox}$ epithelial autophagy-proficient animals. This data supports the hypothesis that *Chlamydia* down-regulates or blocks the completion of host epithelial autophagy, because the cytokine response in wild-type animals infected with *Chlamydia* matched the cytokine response in epithelial autophagy-deficient animals infected with *Chlamydia*, for the cytokines tested.

In order to further explore the implications of autophagy in the pathology of *Chlamydia* infection, we infected a second cohort of animals consisting of p62-deficient mice and wild type mice. P62 is an autophagy protein that acts as a scaffold by associating with ubiquitin-coated bacteria-containing vesicles and LC3-positive isolation membranes. In this way, p62 targets the bacteria for autophagy and allows for specificity within the autophagy immune response [34]. Previous studies have shown that following *Chlamydia* infection, p62 protein expression was either increased or unchanged in human epithelial, mouse fibroblast, and mouse macrophage cell lines [11]. Under normal circumstances, p62 protein is degraded in

the process of autophagy. The increased or unchanged p62 expression in the aforementioned study indicates some blockage to autophagy completion. If autophagy were not blocked at the p62 scaffolding step in *Chlamydia* infection, one would expect to see a decrease of autophagy in p62-deficient *Chlamydia*-infected animals compared to wild type *Chlamydia*-infected animals. Furthermore, one would expect that the decreased ability of p62-deficient animals to launch an autophagy response may result in a more severe pathology compared to wild type infected animals. However, in the current study the bacterial titers in p62-deficient mice and wild type mice showed no significant statistical difference throughout the *Chlamydia* infection. The pathophysiology of the p62-deficient *Chlamydia*-infected mice was similar to the pathophysiology of the wild type *Chlamydia*-infected mice. The cytokine responses to *Chlamydia* infection were similar in both p62-deficient animals and wild type animals for the cytokines that were tested. It is possible that there is redundancy in the autophagy pathway such that another scaffolding protein is upregulated to make up for the lack of p62 protein in p62-deficient animals. Alternatively, autophagy may be blocked by the inability of p62 protein to colocalize with the *Chlamydia* inclusion, which may prevent the bacteria from being directed to the autophagy machinery as suggested by Yasir, et al. [11].

Overall, the results obtained in the current study support the hypothesis that *Chlamydia* evades or down-regulates host epithelial autophagy. In all of the experiments, there were no significant statistical differences between the bacterial titers, pathophysiology, and cytokine responses in autophagy-deficient animals and autophagy-proficient animals infected with *Chlamydia*. The current study may be

strengthened with a larger group of animal test subjects in each of the test groups. For example, in the current study only a small percentage of each group of animals displayed unilateral or bilateral hydrosalpinx following *Chlamydia* infection. It would be particularly interesting to see if a larger test group revealed any significant statistical difference between the pathophysiology of the upper genital tracts of autophagy-deficient and autophagy-proficient animals. Additionally, the results obtained in the current study may be strengthened with a follow-up study that investigates animals with a different component of the autophagy pathway knocked out. Further research is needed to complete the puzzle of *Chlamydia* infection and its interaction with the host autophagy machinery. This research is important for many people worldwide who are impacted by *Chlamydia* infection in order to ultimately find more therapeutic strategies to target *Chlamydia*.

APPENDIX

SPECIFIC METHODS

Procedure for Mouse Intravaginal *Chlamydia* Infection

Materials:

- Medoxyprogesterone
- 20-gauge needle
- Fire-polished 200µL pipette tips
- Sterile 50 mM HEPES buffered to pH 7.4
- Cotton gauze
- EBs for infection, suspended in 2% BSA in SPG solution

Procedure:

1. Seven days before infection, administer medoxyprogesterone subcutaneously, 2.5 mg in 200µl per mouse using a 20-gauge needle.
2. Repeat step 1, three days before infection.
3. Using a fire-polished 200µL pipette tip, rinse each mouse intravaginally with 10µL of sterile 50mM HEPES buffered to pH 7.4.
4. Wipe away excess HEPES buffer with cotton gauze, while holding the mouse tilted on its back.
5. Directly before infection, apply pressure on the bladder of the mouse with gauze to expel any urine and other fluids.
6. Infect at 2 x 10^4 IFU per 10µL/mouse intravaginally using a 200µL fire-polished pipette tip.
7. Discard used tips in the biohazard-sharps container.

Procedure for Swabbing Mice after *Chlamydia* Infection

Materials:

- Swabs
- 2% BSA in SPG solution
- Ice
- Scissors

Procedure:

1. Apply pressure on bladder to expel any fluids and wipe off with gauze.
2. Insert swab into the vagina until hitting the wall. Rotate in a gentle manner for 20 spins.
3. After removing the swab, immediately put it in an eppendorf tube with 500µL 2% BSA in SPG solution.
4. Using scissors cut away the stem of the swab and keep eppendorf on ice until transfer into -80^{o}C.
5. Vortex the intravaginal swab elution and store at -80^{o}C until it is time to perform EB titrations and cytokine assays.
6. Collect swabs after infection on days 3, 7, 10, and then every seven days until day 35.

Procedure for Titrating Elementary Bodies (EBs)

Materials:

- 24-well plate
- Coverslips
- DMEM Medium (10% FCS)
- Cultured HeLa cells
- Swabs from mice infected with *Chlamydia* frozen in 2% BSA in SPG Solution
- Ice-cold methanol

Procedure:

1. Place 1 coverslip in each well of the 24-well plate.
2. Plate HeLa cells on the 24-well plate such that they will grow to _____ cells per well 24 hours later.
3. After 24 hours, perform the following serial dilution with each swab from the infected mice in DMEM:

   Undiluted

   Diluted $1:10^3$

   Diluted $1:10^4$

   Diluted $1:10^5$

   Diluted $1:10^6$

   Diluted $1:10^7$
4. Infect the cells in each well of the 24-well plate with one of the above dilutions.

5. After 24 hours, vacuum media out of each well and fix with 1.5mL of ice-cold methanol.

Procedure for Immunostaining

Materials:

- 24-well plate with titrated EBs
- Microscope slides
- Coverslips
- Ice-cold methanol
- PBS
- Plate shaker
- Mouse anti-MoPn primary antibody
- FITC goat anti-mouse secondary antibody
- Anti-Fade mounting medium
- Immunofluorescence Microscope

Procedure

1. Fix each well of the 24-well plate with titrated EBs with 1.5 mL of ice-cold methanol for 20 minutes or overnight.
2. Rinse the wells three times with PBS.
3. Incubate with mouse anti-MoPn primary antibody for 30 minutes.
4. Rinse the wells three times with PBS.
5. Incubate with the FITC goat anti-mouse secondary antibody for 60 minutes.
6. Rinse the wells three times with PBS.
7. Remove the coverslips from the wells and allow them to air dry.
8. Mount the coverslips on a microscope slide using 3.5μL of Anti-Fade mounting medium.

Procedure for Harvesting Upper Genital Tract

Materials:

- Camera
- Blue background paper
- Ice
- Formalin (10% Formaldehyde)
- 15 mL Falcon tubes
- 70% Ethanol

Procedure:

1. Dissect the upper genital tract from mice 3 months after infection.
2. Place dissected tissue in an empty 15mL Falcon tube and submerge the tube in ice for at least 60 minutes.
3. After 60 minutes on ice, remove tissue from 15 mL Falcon tube and place on Blue background picture.
4. Take pictures of the tissue.
5. Fix the tissue in 15mL formalin for 24 hours.
6. After 24 hours, wash the tissue three times with PBS.
7. Store in 15 mL of 70% ethanol at 4^{o}C.

Procedure for Harvesting Splenocytes

Materials:

- 1mL syringes
- DMEM Medium (10% FCS)
- 70 µL nylon mesh filters
- Centrifuge set at 1200 rpm, 10 minutes, 4°C
- RBC Lysis Buffer
- 24-well plate
- UV-inactivated MoPn EBs

Procedure:

1. Crash the spleen in 70µm nylon mesh using the end of a 1mL syringe in DMEM (10% FCS) medium and collect the splenocytes in a 15mL Falcon tube.
2. Centrifuge at 1200 rpm for 10 minutes at 4°C, and wash the pellet once with DMEM.
3. Centrifuge and discard the supernatant.
4. Resuspend cells in 5 mL of RBC Buffer and incubate for 10 minutes at room temperature.
5. After the 10 minutes, add 5 mL DMEM.
6. Centrifuge and discard supernatant.
7. Wash again with DMEM, centrifuge, resuspend in DMEM
8. Count the cells.

9. Transfer 2 x 10^7 cells into each well of the 24-well plate and add medium to a final volume of 0.5mL per well. Plate duplicate wells for each spleen, one as a control and one for UV-inactivated EB-re-stimulation.

10. Re-stimulate splenocytes with UV-inactivated MoPn at 0.5 x 10^6 IFU per well in 0.5mL.

11. 24 hours after re-stimulation, remove 100 µL of medium for inflammatory cytokine analysis. Store at -80^{o}C.

12. 72 hours after re-stimulation, remove remaining medium in each well for cytokine analysis later. Store at -80^{o}C.

Procedure for Harvesting Blood Sera

Materials:

- 20-gauge needle
- 1 mL syringe
- eppendorf tubes
- centrifuge
- Sodium Azide (NaN_3)

Procedure:

1. Using the 20-gauge needle and 1 mL syringe to remove blood from the heart of the mouse, and put the blood in a 1 mL eppendorf tube.
2. Centrifuge the blood sample for 10 minutes at 1500 rpm.
3. Remove the top, clear serum layer.
4. For long-term storage, add .1% NaN_3 and store at 4^oC.

ELISA Procedure

Materials:

- Biolegend mouse ELISA kits
- ELISA plate reader

Procedure:

1. Follow the BioLegend mouse TNF-alpha, IL-1alpha, IL-4, IL-6, IL-2 ELISA protocols.
2. Use the following dilution of standards for each kit in triplicate.

   500 pg/mL

   250 pg/mL

   125 pg/mL

   62.5 pg/mL

   31.3 pg/mL

   15.6 pg/mL

   7.8 pg/mL

   Blank
3. Read the absorbance at 450 nm and 570 nm.

REFERENCES

1. WHO. 2013 [cited 2013 February 14, 2013]; Available from: http://www.who.int/about/contacthq/en/index.html.

2. press, O.U. *Oxford Dictionaries*. 2013 [cited 2013 February 13]; Available from: http://oxforddictionaries.com.

3. Stephens, R.S., *The cellular paradigm of Chlamydia pathogenesis.* Trends in microbiology, 2003. **11**(1): p. 44-51.

4. Hu, H., G.N. Pierce, and G. Zhong, *The atherogenic effects of Chlamydia are dependent on serum cholesterol and specific to Chlamydia pneumoniae.* J Clin Invest, 1999. **103**(5): p. 747-53.

5. Moazed, T.C., et al., *Murine models of Chlamydia pneumoniae infection and atherosclerosis.* J Infect Dis, 1997. **175**(4): p. 883-90.

6. Wark, P.A., et al., *Chlamydia pneumoniae immunoglobulin A reactivation and airway inflammation in acute asthma.* Eur Respir J, 2002. **20**(4): p. 834-40.

7. Saikku, P., K. Laitinen, and M. Leinonen, *Animal models for Chlamydia pneumoniae infection.* Atherosclerosis, 1998. **140 Suppl 1**: p. S17-9.

8. Balin, B.J., et al., *Identification and localization of Chlamydia pneumoniae in the Alzheimer's brain.* Med Microbiol Immunol (Berl), 1998. **187**(1): p. 23-42.

9. Little, C.S., et al., *Chlamydia pneumoniae induces Alzheimer-like amyloid plaques in brains of BALB/c mice.* Neurobiol Aging, 2004. **25**(4): p. 419-29.

10. Balin, B.J., et al., *Chlamydophila pneumoniae and the etiology of late-onset Alzheimer's disease.* J Alzheimers Dis, 2008. **13**(4): p. 371-80.

11. Yasir, M., et al., *Regulation of Chlamydia infection by host autophagy and vacuolar ATPase-bearing organelles.* Infection and immunity, 2011. **79**(10): p. 4019-28.

12. Heinzen, R.A., et al., *Differential interaction with endocytic and exocytic pathways distinguish parasitophorous vacuoles of Coxiella burnetii and Chlamydia trachomatis.* Infection and immunity, 1996. **64**(3): p. 796-809.

13. Schramm, N., C.R. Bagnell, and P.B. Wyrick, *Vesicles containing Chlamydia trachomatis serovar L2 remain above pH 6 within HEC-1B cells.* Infection and immunity, 1996. **64**(4): p. 1208-14.

14. Scidmore, M.A., E.R. Fischer, and T. Hackstadt, *Restricted fusion of Chlamydia trachomatis vesicles with endocytic compartments during the initial stages of infection.* Infection and immunity, 2003. **71**(2): p. 973-84.

15. van Ooij, C., G. Apodaca, and J. Engel, *Characterization of the Chlamydia trachomatis vacuole and its interaction with the host endocytic pathway in HeLa cells.* Infection and immunity, 1997. **65**(2): p. 758-66.

16. Al-Younes, H.M., T. Rudel, and T.F. Meyer, *Characterization and intracellular trafficking pattern of vacuoles containing Chlamydia pneumoniae in human epithelial cells.* Cellular microbiology, 1999. **1**(3): p. 237-47.

17. Wolf, K., E. Fischer, and T. Hackstadt, *Degradation of Chlamydia pneumoniae by peripheral blood monocytic cells.* Infection and immunity, 2005. **73**(8): p. 4560-70.

18. Yong, E.C., et al., *Degradation of Chlamydia trachomatis in human polymorphonuclear leukocytes: an ultrastructural study of peroxidase-positive phagolysosomes.* Infection and immunity, 1986. **53**(2): p. 427-31.

19. Yong, E.C., E.Y. Chi, and C.C. Kuo, *Differential antimicrobial activity of human mononuclear phagocytes against the human biovars of Chlamydia trachomatis.* Journal of immunology, 1987. **139**(4): p. 1297-302.

20. Deretic, V., *Autophagy in immunity and cell-autonomous defense against intracellular microbes.* Immunological reviews, 2011. **240**(1): p. 92-104.

21. Levine, B., N. Mizushima, and H.W. Virgin, *Autophagy in immunity and inflammation.* Nature, 2011. **469**(7330): p. 323-35.

22. Gutierrez, M.G., et al., *Autophagy is a defense mechanism inhibiting BCG and Mycobacterium tuberculosis survival in infected macrophages.* Cell, 2004. **119**(6): p. 753-66.

23. Gutierrez, M.G., et al., *Autophagy induction favours the generation and maturation of the Coxiella-replicative vacuoles.* Cellular microbiology, 2005. **7**(7): p. 981-93.

24. Pachikara, N., et al., *Productive Chlamydia trachomatis lymphogranuloma venereum 434 infection in cells with augmented or inactivated autophagic activities.* FEMS microbiology letters, 2009. **292**(2): p. 240-9.

25. Chen, L., et al., *Mice deficient in MyD88 Develop a Th2-dominant response and severe pathology in the upper genital tract following Chlamydia muridarum infection.* Journal of immunology, 2010. **184**(5): p. 2602-10.

26. Abdelrahman, Y.M. and R.J. Belland, *The Chlamydia developmental cycle.* FEMS Microbiology Reviews, 2005. **29**(5): p. 949-59.

27. Moulder, J.W., *Interaction of Chlamydiae and host cells in vitro.* Microbiological reviews, 1991. **55**(1): p. 143-90.

28. Eissenberg, L.G. and P.B. Wyrick, *Inhibition of phagolysosome fusion is localized to Chlamydia psittaci-laden vacuoles.* Infection and immunity, 1981. **32**(2): p. 889-96.

29. Eissenberg, L.G., et al., *Chlamydia psittaci elementary body envelopes: ingestion and inhibition of phagolysosome fusion.* Infection and immunity, 1983. **40**(2): p. 741-51.

30. Mizushima, N., T. Yoshimori, and B. Levine, *Methods in mammalian autophagy research.* Cell, 2010. **140**(3): p. 313-26.

31. Lodish, H., *Molecular Cell Biology*. Sixth ed, ed. K. Ahr2008, New York City: W. H. Freeman and Company. 1150.

32. Yu, L., et al., *Termination of autophagy and reformation of lysosomes regulated by mTOR.* Nature, 2010. **465**(7300): p. 942-6.

33. Fujita, N., et al., *The Atg16L complex specifies the site of LC3 lipidation for membrane biogenesis in autophagy.* Molecular biology of the cell, 2008. **19**(5): p. 2092-100.

34. Kuma, A., et al., *The role of autophagy during the early neonatal starvation period.* Nature, 2004. **432**(7020): p. 1032-6.

35. Deretic, V., *Autophagy as an innate immunity paradigm: expanding the scope and repertoire of pattern recognition receptors.* Current opinion in immunology, 2012. **24**(1): p. 21-31.

36. Schmid, D., M. Pypaert, and C. Munz, *Antigen-loading compartments for major histocompatibility complex class II molecules continuously receive input from autophagosomes.* Immunity, 2007. **26**(1): p. 79-92.

37. Dupont, N., et al., *Shigella phagocytic vacuolar membrane remnants participate in the cellular response to pathogen invasion and are regulated by autophagy.* Cell host & microbe, 2009. **6**(2): p. 137-49.

38. Parham, P., *The Immune System*. 3 ed, ed. E. Lawrence2009, New York, NY: Garland Science, Taylor & Francis Group, LLC. 506.

39. Njoku, D.B., *Suppressive and pro-inflammatory roles for IL-4 in the pathogenesis of experimental drug-induced liver injury: a review.* Expert opinion on drug metabolism & toxicology, 2010. **6**(5): p. 519-31.

40. Cotter, T.W., et al., *Reactivation of Chlamydia genital tract infection in mice.* Infection and immunity, 1997. **65**(6): p. 2067-73.

41. de la Maza, L.M., et al., *Intravaginal inoculation of mice with the Chlamydia trachomatis mouse pneumonitis biovar results in infertility.* Infection and immunity, 1994. **62**(5): p. 2094-7.